A&A 530, A21 (2011)
DOI: 10.1051/0004-6361/201016270

Astronomy & Astrophysics

Spectral properties of 438 GRBs detected by *Fermi*/GBM⋆

L. Nava[1], G. Ghirlanda[2], G. Ghisellini[2], and A. Celotti[1]

[1] SISSA, via Bonomea 265, 34136 Trieste, Italy
e-mail: lara.nava@sissa.it
[2] Osservatorio Astronomico di Brera, via E. Bianchi 46, 23807 Merate, Italy

Received 6 December 2010 / Accepted 26 January 2011

ABSTRACT

We present the results of the spectral analysis of the public data of 438 gamma ray bursts (GRBs) detected by the *Fermi* Gamma ray Burst Monitor (GBM) up to March 2010. For 432 bursts we could fit the time-integrated spectrum. In 318 cases we could reliably constrain the peak energy $E^{\rm obs}_{\rm peak}$ of their νF_ν spectrum by analyzing their time-integrated spectrum between 8 keV and 35 MeV. Eighty percent of these spectra are fitted by a power-law with an exponential cutoff, and the remaining with the Band function. Among these 318 GRBs, 274 belong to the long GRB class and 44 to the short. Long GRBs have a typical peak energy $E^{\rm obs}_{\rm peak}$ ∼160 keV and low-energy spectral index $\alpha \sim -0.92$. Short GRBs have a harder peak energy ($E^{\rm obs}_{\rm peak} \sim 490$ keV) and a harder low-energy spectral index ($\alpha \sim -0.50$) than long bursts. For each *Fermi* GRB we also analyzed the spectrum corresponding to the peak flux of the burst. On average, the peak spectrum has a harder low-energy spectral index than the corresponding time-integrated spectrum for the same burst, but similar $E^{\rm obs}_{\rm peak}$. The spectral parameters derived in our analysis of *Fermi*/GBM bursts are globally consistent with those reported in the GRB Cicular Network (GCN) archive after December 2008, while we found systematic differences in the low-energy power-law index for earlier bursts.

Key words. radiation mechanisms: non-thermal – Gamma rays: general

1. Introduction

Our current knowledge of the spectral properties of the prompt emission in GRBs mainly relies on the data collected in almost ten years by the Burst And Transient Source Experiment (BATSE) onboard the Compton Gamma-Ray Observatory (CGRO). BATSE allowed characterization of the spectrum of the population of short and long GRBs over a wide energy range of 20 keV to 1–2 MeV. Analysis of such data revealed some important results about the spectral properties of these GRBs. The prompt spectra, integrated over the GRB duration (i.e. time-integrated spectra), can typically be described well by a curved function showing a peak – in a νF_ν representation – at a typical energy $E^{\rm obs}_{\rm peak}$ of a few hundred keV, but its distribution spans nearly three orders of magnitude. Large dispersions also characterize the distributions of the low – and high – energy photon indices, whose characteristic values are $\alpha \sim -1$ and $\beta \sim -2.3$, respectively (Band et al. 1993; Ghirlanda et al. 2002; Kaneko et al. 2006). Similar results are obtained by considering the time-resolved spectral analysis of flux/fluence limited samples of bright BATSE bursts (Preece et al. 1998, 2000; Kaneko et al. 2006).

The BATSE data also suggest that there are two different classes of GRBs (long and short), based on both temporal and spectral features. Evidence of a spectral diversity between long and short bursts comes from their different hardness-ratios (HR) (Kouveliotou et al. 1993). The higher HR of short bursts might be ascribed to a larger $E^{\rm obs}_{\rm peak}$. Nava et al. (2008) and Ghirlanda et al. (2009 – G09 hereafter) showed that $E^{\rm obs}_{\rm peak}$ correlates both with the fluence and the peak flux. Although short and long bursts follow the very same $E^{\rm obs}_{\rm peak}$-peak flux relation, they obey different (parallel) $E^{\rm obs}_{\rm peak}$-fluence relations. This obviously implies that the distributions of the ratio $E^{\rm obs}_{\rm peak}$/fluence is different for the two burst classes. Recently, Goldstein et al. (2010) have proposed this ratio as a discriminator between short and long GRBs. Owing to the relation between $E^{\rm obs}_{\rm peak}$ and the bolometric fluence and peak flux, a direct comparison between the $E^{\rm obs}_{\rm peak}$ distributions of the two different burst classes must take the different fluence/peak flux selection criteria into account. G09 analyzed and compared samples of short and long BATSE bursts selected with similar peak flux limits. They found that the peak energy distributions of the two classes are similar, while the most significant difference is in the low-energy power-law indices, with short bursts typically having a harder $\alpha \sim -0.4$.

These global spectral properties of GRBs have also been confirmed by other satellites (*Beppo*SAX, Hete-II and Swift) (Guidorzi et al. 2010; Sakamoto et al. 2005; Butler et al. 2007). However, the detectors onboard these satellites have different sensitivities than BATSE and cover a narrower and different energy range. For instance, the relatively narrow energy range (15–150 keV) of Swift/BAT does not allow the spectral peak $E^{\rm obs}_{\rm peak}$ to be constrained for most of the detected bursts (Cabrera et al. 2007; Butler et al. 2007).

Spectral studies of the prompt emission of GRBs require a wide energy range, possibly extending from a few tens of keV to the MeV energy range. This allows a measure of the curvature of the GRB spectrum and constraining its peak energy, as well as its low-and high-energy spectral slopes.

The *Fermi* satellite, launched in June 2008, represents a powerful opportunity to shed light on the origin of the GRB prompt

⋆ Tables 2–5 are available in electronic form at http://www.aanda.org

emission thanks to its two instruments: the Large Area Telescope (LAT) and the Gamma-ray Burst Monitor (GBM). LAT detected very high-energy emission (>100 MeV) from 19 GRBs in about two years. This emission component shares some common features with what has already been found in a few bursts by EGRET (Energetic Gamma-Ray Experiment Telescope) onboard the CGRO satellite. In particular, high-energy ~GeV flux is still observed when the softer energy emission (in the sub-MeV domain) ceases, and often its onset lags the sub-MeV component (e.g. Ghisellini et al. 2010; Omodei et al. 2009).

The other instrument onboard *Fermi* is the GBM (Meegan et al. 2009), which is similar to BATSE and, despite its slightly worse sensitivity, allows study of the GRB spectrum over an unprecedentedly wide energy range, from 8 keV to 40 MeV. This is achieved by its twelve NaI detectors, giving a good spectral resolution between ~8 keV and ~1 MeV and two BGO detectors, which extend the energy range up to ~40 MeV. Similar to BATSE, the NaI detectors guarantee full-sky coverage, but their smaller geometric area (16 times lower than that of the LADs of BATSE) implies a lower sensitivity. On the other hand, the presence of the BGO detectors allows the energy range to be extended for the first time for the study of the spectrum of the prompt emission to tens of MeV, thus accessing an energy range that is poorly explored with the CGRO instruments.

438 events, classified as GRBs[1], triggered the GBM until the end of March 2010. *With this large sample of bursts we can perform the first robust statistical study of the spectral properties of Fermi/GBM bursts*. The main aims of this paper are (a) to present the results of the spectral analysis of 438 *Fermi* bursts, (b) to show the distribution of their spectral parameters, (c) to compare the spectral properties of *Fermi* short and long GRBs, and (d) to compare the spectra integrated over the burst duration (time-integrated spectra, hereafter) with the spectra of the most intense phase of the burst, i.e. its peak flux (peak spectra, hereafter).

Preliminary results of the spectral analysis of *Fermi* GRBs performed by the GBM team have been distributed to the community through the Galactic Coordinates Network (GCN) circulars. These amount to 228 GRBs (until March 2010), whereof 167 have a well constrained $E^{\rm obs}_{\rm peak}$. Ongoing spectral calibrations of the GBM detectors mean that the results published in the GCN are "preliminary", especially for the first bursts detected by the GBM. The GBM team continuously provides more updated detector response files, together with the public data of detected GRBs. A few months ago the software and the new response files were made public so that a systematic and reliable analysis of the spectra of *Fermi*/GBM bursts is now possible. We compare the results of our spectral analysis with those published in the GCN to search for possible systematic effects in the GCN results.

The paper is organized as follows. In Sects. 2 and 3 we describe the sample of *Fermi* GRBs and the procedure adopted to extract and analyze their spectral data. In Sect. 4 we present the spectral results and build their distributions, while considering short and long GRBs separately. In Sect. 4 we also compare the time-integrated spectra and the peak spectra for the analyzed bursts. We summarize our results in Sect. 5.

[1] http://heasarc.gsfc.nasa.gov/W3Browse/fermi/fermigbrst.html

2. The sample

The GBM detected 438 GRBs up to the end of March 2010. A list of the GRB trigger number and the position in the sky, computed by the GBM, is provided by the Fermi Science Support Center[1]. The data of each GRB have been archived and made public since July 2008. Since the only information given in the public archive is the burst position, it was not possible to apply any selection in flux, fluence, or duration on the GBM online public archive, since a spectral catalog is not available. For this reason we started the systematic analysis of GBM bursts in order to determine the spectral parameters, fluence, and peak flux of all bursts detected by *Fermi*/GBM up to March 2010.

Preliminary spectral results of *Fermi* GRBs have been distributed by the GBM team through the GCN system. Starting on March 2010, the number of GCN of *Fermi* bursts substantially decreased, although the rate of detected bursts remained unchanged. We decided to limit our selection to March 2010, thus having a large sample of GCN results to compare with.

We collected all bursts with spectral information published in the GCN up to the end of March 2010 (228 objects). Among these, 148 long GRBs and 19 short have well-constrained spectral parameters, in particular the peak energy of their νF_ν. In Sect. 4 we compare the GCN spectral parameters with those derived by us for the same bursts and search for possible systematic effects in the GCN results.

3. Spectral analysis

For the spectral analysis of *Fermi*/GBM bursts we used the recently released `rmfit` – v3.3pr7 software[2]. For each GRB to be analyzed, the spectral analysis was done by combining together more than one detector. Following the criterion adopted in Guiriec et al. (2010) and Ghirlanda et al. (2010), we selected the most illuminated NaI detectors having an angle between the source and the detector normal lower than 80 degrees. We selected the BGO #0 or #1 if the selected NaI were all between #0-5 or #6-12, respectively. When the selected NaI were both between #0-5 and #6-12, both BGO detectors were used. However, if one of the two BGO had a zenith angle to the source larger than 100 degrees we excluded it from the analysis.

The very wide available energy range (from 8 keV to ~40 MeV) allows proper constraining of the peak energy of particularly hard GRBs (with $E^{\rm obs}_{\rm peak}$ larger than 1 MeV, i.e. the upper energy threshold of the NaI detectors) or the high-energy spectral power law, if present.

For the spectral analysis we used the CSPEC data (with time resolution of 1.024 s after the trigger time and 4.096 s before) for long GRBs and the TTE data (with time resolution of 0.064 s) for short GRBs. A first hint about the burst duration comes from the visual inspection of the lightcurves (at different temporal resolutions) stored in the quicklook directory provided with the data[1]. We used this method to decide which type of data (CSPEC or TTE) is more suitable for spectral analysis. Both data types contain spectra with 128 energy channels. Following the prescription of the `rmfit` tutorial[3] we considered the spectral data of the NaI detectors in the range 8 keV–900 keV and for the BGO detectors in the range 250 keV–35 MeV.

For each GRB we extracted the background spectrum by selecting a time interval before and after the burst that was as large

[2] http://fermi.gsfc.nasa.gov/ssc/data/analysis/

[3] http://fermi.gsfc.nasa.gov/ssc/data/analysis/user/vc_rmfit_tutorial.pdf

as possible, but distant enough from the burst signal to avoid burst contamination. The spectra in these two time intervals were modeled in time with a polynomial of order between 0 and 4 to account for the possible time evolution of the background. Then, the spectral analysis software extrapolates the background to the time interval occupied by the burst. We used the most updated response files with extension rsp2, which allows rmfit to use a new response for each 5 deg of spacecraft slew, as explained in the rmfit tutorial.

Each spectrum was analyzed by adopting the Castor statistics (C-stat). Since we combined NaI and BGO detectors in the spectral analysis, we fitted the spectra by allowing for a calibration constant among the different detectors. The spectral results (C-stat and spectral parameters) obtained with the calibration constants free and fixed to 1 were compared. If no significant difference was found between the C-stat and the spectral parameters obtained in these two cases, the calibration constants were fixed to 1 (as also suggested in the rmfit manual). In nearly 30% of the cases, the C-stat significantly decreased by using free calibration constants. This is not directly related to the burst brightness (also for faint bursts the calibration constants can be required) even if, of course, the largest differences in C-stat values are found for bright bursts, since possible calibration offsets between instruments strongly affect the fit (in terms of C-stat) when data points have small errors.

Systematic residuals around the k-edge of the NaI detectors are often visible, owing to calibration issues (Guiriec et al. 2010). For four bursts (for which this effect is particularly pronounced), we performed the spectral analysis both including and excluding a few channels between 30 keV and 40 keV (e.g. see Guiriec et al. 2010). While the spectral parameters and their errors are not sensitive to this choice, the value of the C-stat is quite different. For these four bursts we report the results of both the analyses (Table 2).

3.1. Spectral models

The spectral analysis performed by different authors (Preece et al. 2000; Sakamoto et al. 2005; Kaneko et al. 2006; Butler et al. 2007; Nava et al. 2008; Guidorzi et al. 2010) on data taken from different instruments revealed that GRB spectra are fitted by different models, the simplest ones being i) a single power-law model (PL), ii) a Band function (Band et al. 1993), which consists of two smoothly connected power-laws and iii) a Comptonized model (CPL hereafter), i.e. a power-law with a high-energy exponential cutoff.

The time-resolved spectra of BATSE GRBs have been also fitted by combining thermal (black-body) and nonthermal (power-law) models (e. g. Ryde et al. 2005; Ryde et al. 2009). Although these fits are intriguing for their possible physical implications (Pe'er et al. 2010), they are statistically equivalent to fits with the phenomenological models described above (Ghirlanda et al. 2007). Recently, Guiriec et al. (2010) have found evidence of a thermal black body component (summed to the standard Band function) in the spectrum of the Fermi GRB 100724B.

A simple PL function clearly indicates that no break/peak energy is detected within the energy range of the instrument. Furthermore, it is also statistically the best choice when the signal-to-noise ratio of the analyzed spectra is very low because this model has the lowest number of free parameters. This was shown, for instance, by the analysis of the Swift/BAT spectral data (e.g. Cabrera et al. 2007).

The Band model (Band et al. 1993) has four free parameters to describe the low and high power law behaviors, the spectral break and the flux normalization. Typically, the low-energy photon index $\alpha > -2$ [$N(E) \propto E^{\alpha}$] and the high-energy photon index $\beta < -2$ [$N(E) \propto E^{\beta}$], so that a peak in νF_{ν} can be defined. When there is no evidence of a high-energy photon tail or $E^{\rm obs}_{\rm peak}$ is near the high-energy boundary of the instrument sensitivity (and β is poorly constrained), a CPL model is preferred due to the lower number of parameters. Also in this case a peak energy can be defined when $\alpha > -2$. In the Band model the spectral curvature is fixed by α, β, and $E^{\rm obs}_{\rm peak}$.

We fitted all these nested models to each GRB spectrum. The addition of one free parameter requires an improvement in C-stat of 9 for a 3σ confidence in this improvement. We chose this criterion to select the best-fit model. In addition, we also required that all the spectral parameters are well determined (i.e. no upper or lower limits).

3.2. Time integrated and peak flux spectra

As anticipated we analyzed, for each burst, (1) the spectrum integrated over its whole duration and (2) the spectrum corresponding to the peak of the burst. For the peak spectrum, this could be selected from the raw-count light curve as the temporal bin with the highest count rate. However, it may happen that bins with a similar count rate have very different spectra, and their flux can be considerably different. Therefore, a more physical approach for identifying the peak of the burst is to build its flux light curve (i.e. calculating the flux in physical units). In practice, we performed a time-resolved spectral analysis of each burst and built its flux light curve, where the flux is integrated over the 8 keV–35 MeV energy range, i.e. the same spectral range where the spectral analysis is performed). Then we identified the time bin corresponding to the largest flux and analyzed this spectrum to extract the peak spectrum parameters. As timescale for the time-resolved spectral analysis, we chose 1.024 and 0.064 seconds for the long and short GRBs, respectively. We adopt this procedure for all GRBs, i.e. even those having a time-integrated spectrum better described by a simple power-law.

4. Results

The spectral parameters obtained from analysis of the time-integrated spectra of the 438 *Fermi*/GBM bursts are reported in Tables 2 and 3. In particular, in Table 2 we list all the 323 bursts whose spectrum could be fitted with either the Band or CPL model (Col. 3). In five cases, the high-energy power-law index β is >-2, and this reduces the number of bursts with well-defined peak energy $E^{\rm obs}_{\rm peak}$ to 318. In Table 3 we report all the 109 cases where a single power-law is the best fit to the data and the 6 cases where spectral analysis was impossible for lack of data.

In both tables we give the time interval over which the time-integrated spectrum was accumulated and the best-fit model (Cols. 2, 3), the normalization constant (Col. 4) in units of photons cm^{-2} s^{-1} (computed at 100 keV for all models), and the spectral index α (Col. 5) of the low-energy power-law. The peak energy of the νF_{ν} spectrum and (for the spectra fitted with the Band model) the high-energy spectral index β are listed in Cols. 6 and 7 of Table 2, respectively. We also report in both tables the value of the C-stat resulting from the fit and the associated degrees of freedom (d.o.f.). The last column in Table 2 gives the fluence obtained by integrating the best-fit model over the 8 keV–35 MeV energy range. For the spectra fitted with

the PL model, we give the fluence (last column in Table 3) computed over a narrower energy range, 8 keV–1 MeV, because we could not identify where the peak energy is. For four bursts (GRB 081009140, GRB 090618353, GRB 090626189, and GRB 090926181), we performed the spectral analysis both including and excluding a few channels around the k-edge. In these cases, we report both the results in the tables. In 19 cases we found that the fit with a Band model returns well constrained parameters, but it is not statistically preferred to the Comp model (the C-stat improvement is lower than 9). In these cases we list the parameters of both models in the tables.

In Table 4 we report the results of the peak spectra analysis. In particular, we list the initial (t_1) and final (t_2) times of the selected temporal bin, the best-fit model, its spectral parameters, C-stat, and degrees of freedom. The last column lists the peak flux estimated in the 8 keV–35 MeV energy range. Finally, in Table 5, we list the spectral properties and the fluence collected from the GCN Circulars. For each burst we also report the redshift (when available) and the GCN number.

4.1. Time-integrated spectra

Out of the 432 bursts for which it was possible to perform the spectral analysis, 359 are long and 73 short. In the case of long (short) bursts, 274 (44) events have a well-defined peak energy, while 4 (1) are best fitted with a Band model with $\beta > -2$. Most of the spectra are adequately fitted by the CPL model. This is true for both the long and short subgroups. Among the 109 spectra fitted with a simple power-law model, there are 81 and 28 long and short events.

In our analysis we integrated the spectrum over a time interval (ΔT) where the signal of the burst (for all NaI detectors combined) is stronger than the average background. Therefore, we adopt this integration time to separate short and long GRBs (i.e. $\Delta t < 2$ s and $\Delta t > 2$ s, respectively). The distribution of Δt is bimodal and short and long GBM bursts are separated into two log normal distributions with central value (standard deviation) $\langle \mathrm{Log}(\Delta t)\rangle = 1.42$ ($\sigma = 0.39$) and $\langle \mathrm{Log}(\Delta t)\rangle = -0.33$ ($\sigma = 0.38$) for long and short GRBs, respectively.

Fluence distribution – In Fig. 1 we show the Log$N$ – Log$F$ distributions of the *Fermi* GRBs analyzed. To show the fluence distribution of all the 432 GRBs that we could successfully fit, we computed the fluence in the 8 keV–1 MeV for the 323 GRBs fitted with either the Band or CPL model and for the 109 GRBs fitted with a power-law. We show separately the Log$N$–Log$F$ for long (359 events) and short (73 events) GRBs. At large fluences the distribution of long and short has a very similar slope to the euclidean one (–3/2), which is shown for comparison. In Fig. 2 we show the Log$N$ – Log$F$ distribution by dividing our sample according to the best-fit model.

$E_{\rm peak}$ distribution – In Fig. 3 we show the peak energy distribution of the 318 GRBs (both long and short) and the fit with a Gaussian. Also, in Fig. 3 short and long events are shown separately and the Kolmogorov-Smirnov test gives a probability $P_{\rm KS} = 3.4 \times 10^{-15}$ that the two distributions of $E^{\rm obs}_{\rm peak}$ for long and short GRBs are drawn from the same parent distribution.

Spectral index distributions – In Fig. 4 we show the distribution of the low-energy spectral index α for all the 318 GRBs and for short and long GRBs separately (having a $P_{\rm KS} = 7.3 \times 10^{-12}$). Finally, in Fig. 5 we show the distribution of the high-energy spectral index β for the 60 time-integrated spectra that are fitted with the Band model (see Table 2).

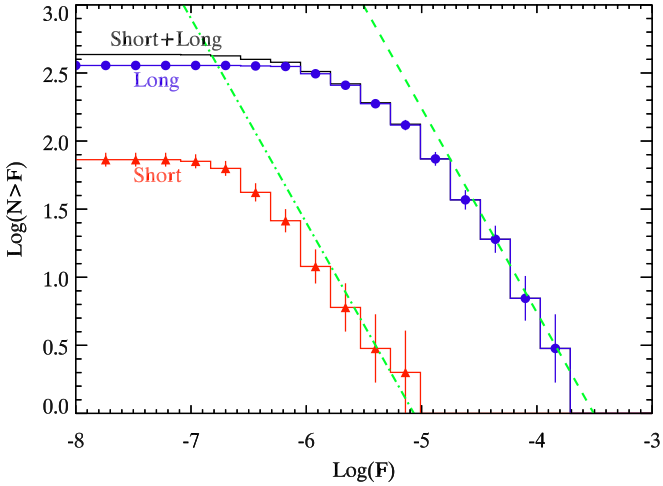

Fig. 1. Log$N$ – Log$F$ of the 432 GRBs analyzed in this work (Tables 2 and 3). Short GRBs (73 events) and long GRBs (359 events) are shown with (red) triangles and (blue) circles, respectively. The black histogram refers to the entire sample. The dashed and dot-dashed lines are two power-laws with slope –3/2. The fluence F in erg/cm^2 is obtained by integrating the best-fit model in the 8 keV–1 MeV energy range.

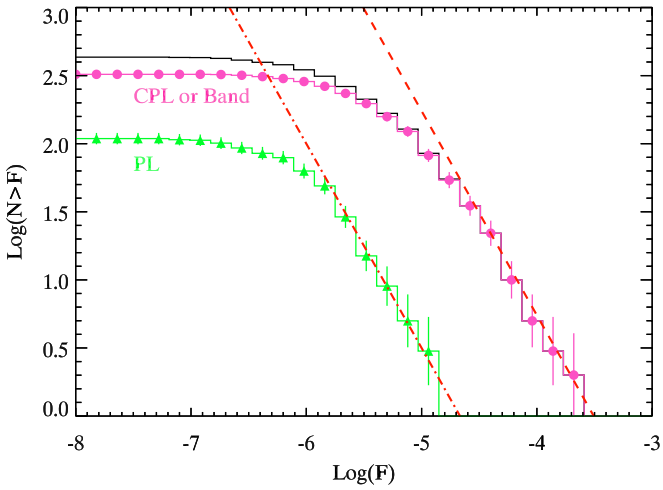

Fig. 2. Log$N$ – Log$F$ distributions of all the GRBs fitted with the CPL or Band model and well-constrained $E^{\rm obs}_{\rm peak}$ (pink circles) and of the 109 GRBs fitted with a single PL model (green triangles). For reference a power law with slope –3/2 is shown (dashed and dot-dashed line). The fluence F in erg/cm^2 is obtained by integrating the best-fit model in the 8 keV–1 MeV energy range.

All the parameters distributions shown in Figs. 3 and 4 are fitted by Gaussian functions whose parameters are reported in Table 1.

4.2. Peak spectra

For each burst we also extracted and analyzed the spectrum corresponding to its peak flux. To this aim, we performed a time-resolved spectral analysis of each burst. In the flux light curve, we then selected the time bin with the largest flux. The timescale is given by the resolution of the data, i.e. typically 1.024 s and 0.064 s for long and short GRBs, respectively. We also verified that in most cases the peak of the count rate coincides with the peak of the flux.

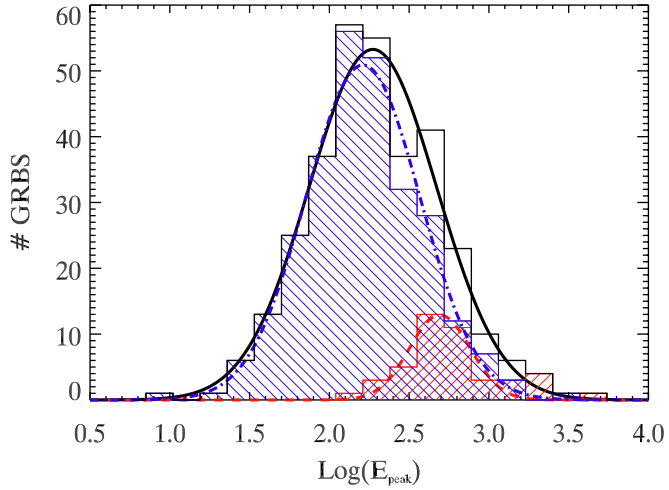

Fig. 3. Distribution of the peak energy for the GRBs listed in Table 2 fitted with either the Band or CPL model and with determined $E^{\rm obs}_{\rm peak}$ (318 GRBs). The solid line shows the fit with a Gaussian. Also shown (hatched blue and red histograms) are the distributions for 274 long and 44 short GRBs, respectively, and their Gaussian fits (dot-dashed and dashed lines for long and short events, respectively).

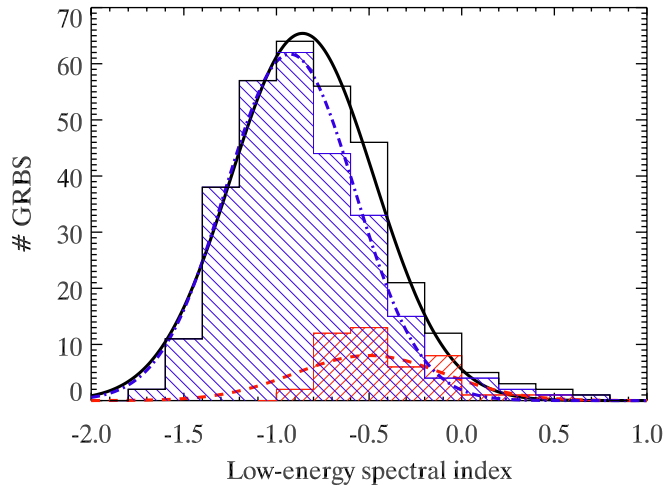

Fig. 4. Distribution of the low-energy photon index for the 318 GRBs listed in Table 2 fitted with either the Band or CPL model and with determined $E^{\rm obs}_{\rm peak}$. The solid (black) line shows the fit with a Gaussian. Also shown (hatched blue and red histograms) are the distributions for 274 long and 44 short GRBs, respectively, and their Gaussian fits (dot-dashed and dashed line for long and short events, respectively).

Out of the 432 analyzed GRBs, the peak spectrum could be extracted and fitted with a Band or CPL model in 235 cases. As before, the best-fit model is defined by requiring an improvement in the C-stat value of 9 (between a given model and a more complex one with one parameter more) and well-constrained spectral parameters. In 27 cases (26 long and 1 short) the best-fit model of the peak spectrum is different from that of the time-integrated spectrum. The spectral parameters of the peak spectra fitted with these two models are reported in Table 4.

In Fig. 6 we compare the peak energy $E^{\rm obs}_{\rm peak}$ and the low spectral index α at the peak flux with the values of the time-integrated spectrum for bursts having all this information (227 events.). Empty (filled) symbols refer to GRBs for which the time-integrated and the peak spectra are described by the same (a different) best-fit model. On average, the time-integrated and peak

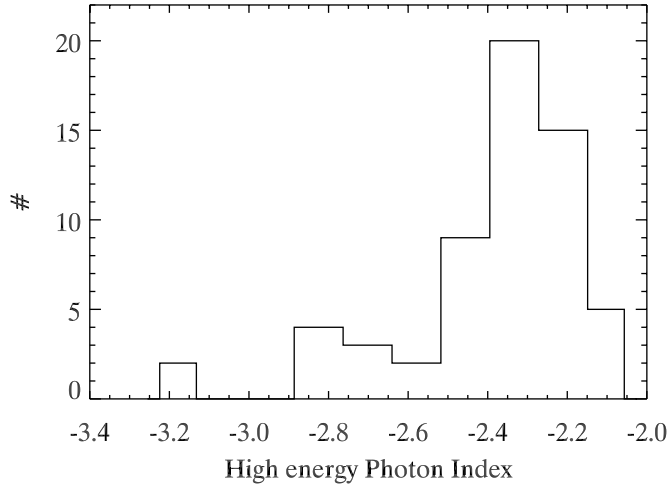

Fig. 5. Distribution of the high-energy photon index for 60 GRBs whose time-integrated spectrum is best fit with the Band model.

Table 1. Parameters of the Gaussian fits of the distributions of the spectral parameters of *Fermi*/GBM bursts analyzed in this work.

Parameter	Type	# of GRBs	Central value	σ
Log($E^{\rm obs}_{\rm peak}$)	All	318	2.27	0.40
	Short	44	2.69	0.19
	Long	274	2.21	0.36
α	All	318	–0.86	0.39
	Short	44	–0.50	0.40
	Long	274	–0.92	0.35

spectrum values of $E^{\rm obs}_{\rm peak}$ are very similar, while the low-energy spectral index, at the peak, is harder.

4.3. Comparison with GCN results

Since August 2008, the Fermi GBM team is providing preliminary results of the spectral analysis of a large number of the detected GRBs through the GCN Circulars. For each burst, the GCN circular reports the burst's duration, spectral parameters, fluence, and photon peak flux (all with their associated errors). GCN circulars are promptly released when a burst occurs and are not updated after their first release. On the other hand, the GBM team is continuously providing, through the online archive, new versions of the detector response files, improved with respect to the first version used to perform their preliminary analysis. Our analysis benefits from the most updated response files. A meaningful comparison between our results and those preliminarily reported by the GBM team must account for this difference.

It is likely that the calibration of the different detectors has changed and been improved from the earliest to the latest circular, along with the software and tools used by the Fermi team. If this is the case, spectral parameters of the first bursts detected by Fermi and reported in the GCN could be affected by systematic biases, hopefully not present in our analysis. To verify this possibility, we plotted the spectral parameters (α and $E^{\rm obs}_{\rm peak}$) as a function of the date (in MJD) of the GRB detection, to point out any possible systematic trend of their values and/or associated uncertainties. The spectral parameters (from our sample and from the GCN sample) are plotted in the upper panels of Fig. 7.

In the GCN sample, long bursts (Fig. 7) detected at the beginning of the mission have a slightly harder α with respect to

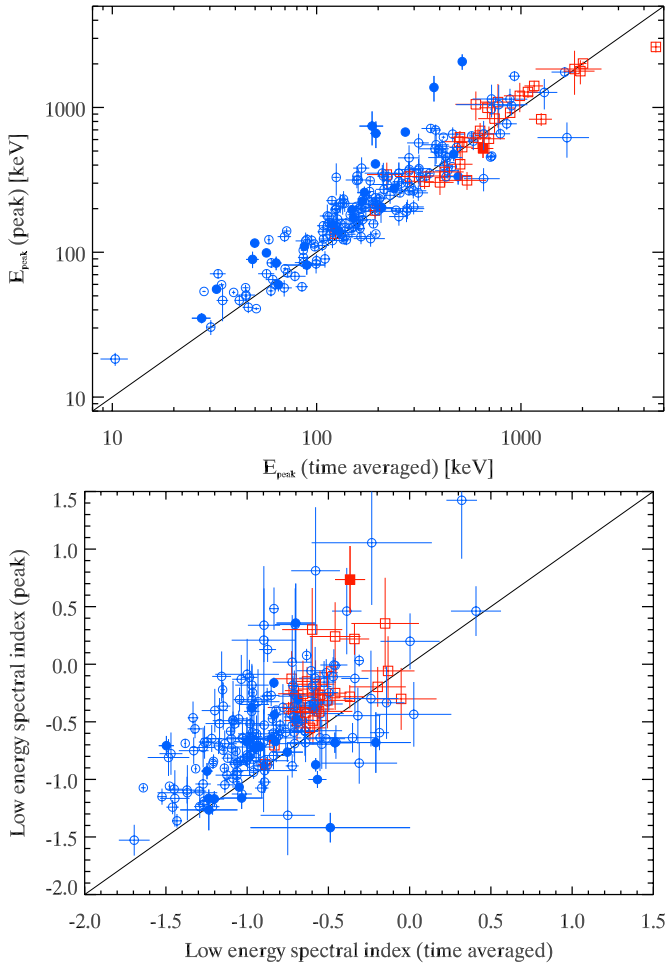

Fig. 6. Comparison of time-integrated and peak-flux spectral parameters for the 227 GRBs whose peak spectrum could be fitted with the Band or CPL model (reported in Table 4 and present also in Table 2). *Top panel*: peak energy. *Bottom panel*: low-energy spectral index (α). Empty (filled) symbols are GRBs for which the time-integrated and the peak flux spectra have same (different) best fit model. Squares refer to short events and circles to long events.

the following bursts and also to the same bursts analyzed by us. This trend is not present in the short burst sample. In this case, however, the sample is small, and short bursts are only present in the GCN sample starting from December 2008.

A possible bias on the α values can be better quantified by probing how the α distribution for long bursts evolves in time. After having sorted GRBs according to their increasing date of detection, we consider the distribution of the spectral parameter up to a certain date and we fit it with a Gaussian function by deriving its central value and the standard deviation. This corresponds to showing how the *cumulative* distributions change by increasing the time span. Since a systematic difference in α between our analysis and what is reported in the GCNs might also be ascribed to a systematic difference in the choice of the best-fit model, we use only those bursts for which the best-fit model is the same in both analyses.

Our test starts on November 2008, when we start to have enough bursts for a reliable Gaussian fit. The middle left panel in Fig. 7 shows our results. The y-axis shows the central value of the Gaussian fit and the error bar correspond to its 1σ width. In the GCN sample a trend is clearly visible. Although at the 1σ level we see that all the central values are consistent, the mean of α (~ -0.5 at the beginning) systematically evolves from harder to softer values, and then it levels off at about –0.85. This result rules out the possibility that the bias is due to a different choice in the best-fit model and suggests that another nonphysical effect could be biasing the low-energy power-law indices towards harder values in the first months of the GCN data analysis. This trend is not present in our sample (Fig. 7, middle left panel), for which the α distribution does not evolve in time.

The whole α distributions for the two different samples are somewhat different, with the GCN sample having slightly harder spectral indices ($\langle\alpha\rangle = -0.86$ compared to $\langle\alpha\rangle = -0.92$ derived from our analysis), as shown by the last point in the middle-left panel of Fig. 7. We are interested in understanding whether this difference can be totally ascribed to the bias affecting the first bursts and, in this case, in determining the date from which GCN preliminary results are consistent with those obtained by our analysis with the most updated response files. The bottom panels of Fig. 7 show the average values of α and $E^{\rm obs}_{\rm peak}$ for two different periods of time: up to the end of December 2008 and from January 2009 to March 2010.

Figure 8 shows the difference $\Delta\alpha$ between the low-energy spectral indices as reported in the GCN sample and as derived by us for bursts common to both samples. The upper panel shows bursts fitted with the same best-fit model in both analyses (i.e. the same subsample as used in Fig. 7). The bottom panel, instead, shows all bursts common to both samples. Approximately up to the end of December 2008, this difference is not randomly distributed around $\Delta\alpha = 0$, but is systematically larger. This justifies our choice of considering these two time intervals for the bottom panels of Fig. 7, showing that bursts in the GCN sample up to the end of December 2008 have a mean $\alpha = -0.5$, while the α distribution of the remaining bursts is peaked around $\alpha = -0.9$, perfectly consistent with our results. The same separation has been applied to our sample, which does not show any difference in α when comparing bursts before and after December 2008 (bottom left panel in Fig. 7).

The $E^{\rm obs}_{\rm peak}$ values (right panels in Fig. 7) are untouched by this effect. The results from the two different samples are highly consistent. A weak trend is visible, but the central value of the $E^{\rm obs}_{\rm peak}$ distribution spans 130 keV to 150 keV, a very narrow range if compared to the width of the distribution and to the typical errors on this parameter.

5. Summary and conclusions

We analyzed the spectra of all GRBs detected by the *Fermi*/GBM between 14 July 2008 and 30 March 2010. There are 438 GRBs, and for 432 of them we have all the data needed to perform the spectral analysis. The time-integrated spectrum is best fitted with a power-law model (110 spectra-reported in Table 3) or a curved model (323 spectra – reported in Table 2), which is either the Band model (65 spectra) or a cutoff-power-law (CPL) model (258 spectra).

Among the 432 GRBs for which we could analyze the spectrum, we identify 73 short and 359 long bursts. Their Log$N$ – Log$F$ is similar (Fig. 1) and its high-fluence tail is consistent with a power law with slope –3/2.

The 73% of the bursts detected by the GBM up to March 2010 could be fitted with a curved model (Band or CPL, with a prevalence of the latter model) and in the majority (318 out of 323) of these cases we could constrain the spectral parameters, in particular, the peak energy $E^{\rm obs}_{\rm peak}$ of the νF_ν spectrum. This is possible thanks to the wide energy range of the GBM spectra

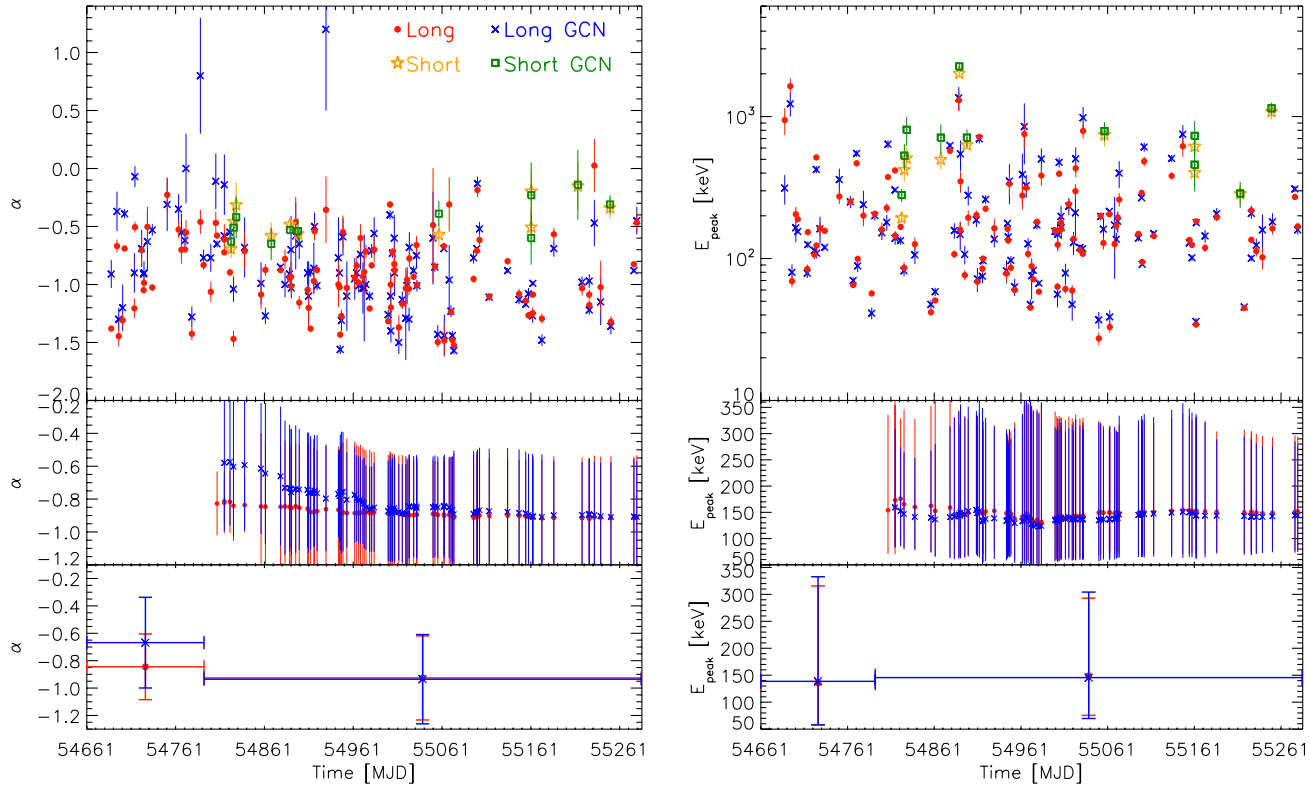

Fig. 7. Comparison of GCN preliminary results and our analysis. *Upper panel*: crosses and squares show (for long and short events respectively) the time trend of the spectral properties (α on the *left* and $E^{\rm obs}_{\rm peak}$ on the *right*) for GBM bursts whose preliminary spectral analysis has been reported in the GCN circulars. Circles and stars show the same for the sample of long and short bursts analyzed by us. We show only those bursts for which the same spectral models were used in our analysis and in the analysis reported in the GCN circulars. Time on the x-axis is in MJD units. *Middle panels*: central values and 1σ width for the α (*left*) and $E^{\rm obs}_{\rm peak}$ (*right*) distributions (long bursts only) for the GCN sample (crosses) and our sample (circles) as a function of time. *Bottom panels* show the average α and $E^{\rm obs}_{\rm peak}$ for two different periods of time, up to and after December 2008.

extending from 8 keV to ~35 MeV. This is the sample we considered for characterizing the spectral parameters of the time-integrated spectra of *Fermi* GRBs. Within this sample there are 44 short and 274 long GRBs. The comparison of their spectral properties shows that short GRBs have higher $E^{\rm obs}_{\rm peak}$ than do long events (Fig. 3) and a slightly harder low-energy spectral index α (Fig. 4).

The finding that short *Fermi* GRBs have harder peak energy than long events seems opposite to what has been found from the comparison of short and long GRBs detected by BATSE (Ghirlanda et al. 2009).

However, the *Fermi* short GRBs also have larger peak fluxes than long events. A more detailed comparison between long and short GRBs detected by *Fermi*/GBM and BATSE is presented in Nava et al. (2010).

A second major part of the present work was to characterize the spectra of the peak of each GRB. Through time-resolved spectroscopy, we isolated and analyzed the spectrum corresponding to the peak of the flux light curve of each burst. The results are reported in Table 4. By comparing the peak spectrum and the time-integrated spectrum of individual GRBs, we find that the peak spectra have similar $E^{\rm obs}_{\rm peak}$ of the time-integrated spectra but harder low-energy spectral index α (Fig. 6).

Finally we compared the results of our spectral analysis with those reported in the GCN circulars. We found that the still not fully completed calibrations of the GBM detectors means that the GCN results of bursts comprised between July and December 2008 are affected by a systematic overestimate of the hardness of the GRB spectrum at low energies (i.e. the spectral parameter α).

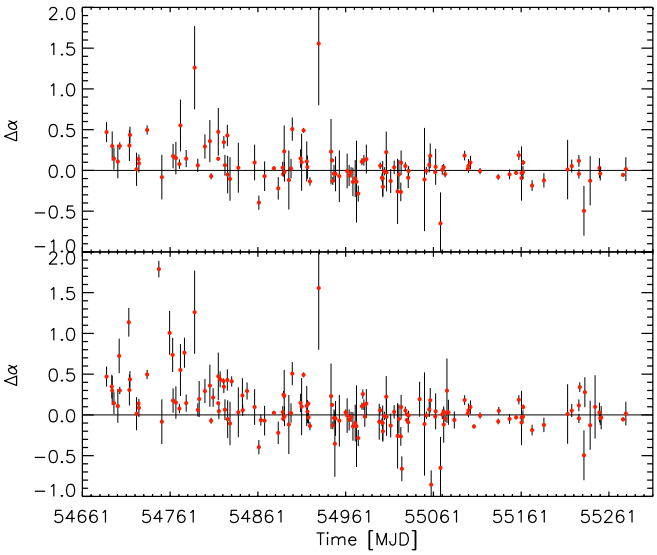

Fig. 8. Difference between α values reported in the GCN Circulars and α values derived from our analysis. *Top panel*: bursts for which the spectrum is described by the same model both in our analysis and in the GCN analysis. *Bottom panel*: bursts common to both samples regardless of the spectral model chosen to describe the spectrum.

This systematic bias does not affect $E^{\rm obs}_{\rm peak}$ and is not present in our results, which were obtained with the most recent releases of the GBM response files.

Acknowledgements. This research has made use of the public *Fermi*/GBM data and software obtained through the High Energy Astrophysics Science Archive Research Center Online Service, provided by the NASA/Goddard Space Flight Center. We acknowledge the GBM team for the public distribution of the spectral properties of *Fermi*/GBM bursts through the GCN network. We thank the referee for his/her useful comments. This work has been partly supported by ASI grant I/088/06/0. L.N. thanks the Osservatorio Astronomico di Brera for the kind hospitality for the completion of this work.

References

Band, D., Matteson, J., Ford, L., et al. 1993, ApJ, 413, 281
Berger, E., Fox, D. B., & Cucchiara, A. 2008, GCN, 8335
Bhat, P. N. 2009, GCN, 8899
Bhat, P. N. 2009, GCN, 8911
Bhat, P. N. 2009, GCN, 9020
Bhat, P. N. 2009, GCN, 9311
Bhat, P. N. 2009, GCN, 9427
Bhat, P. N. 2009, GCN, 9428
Bhat, P. N. 2009, GCN, 9429
Bhat, P. N., & van der Horst, A. J. 2008, GCN, 8552
Bhat, P. N., & van der Horst, A. J. 2008, GCN, 8589
Bhat, P. N., Paciesas, W., & van der Horst, A. J. 2008, GCN, 8205
Bhat, P. N., Preece, R. D., & van der Horst, A. J. 2008, GCN, 8550
Bissaldi, E. 2008, GCN, 8370
Bissaldi, E. 2008, GCN, 8551
Bissaldi, E. 2008, GCN, 8720
Bissaldi, E. 2009, GCN, 8917
Bissaldi, E. 2009, GCN, 9119
Bissaldi, E. 2009, GCN, 9294
Bissaldi, E. 2009, GCN, 9295
Bissaldi, E. 2009, GCN, 9486
Bissaldi, E. 2009, GCN, 9497
Bissaldi, E. 2009, GCN, 9511
Bissaldi, E. 2009, GCN, 9523
Bissaldi, E. 2009, GCN, 9608
Bissaldi, E. 2009, GCN, 9742
Bissaldi, E., & Connaughton, V. 2009, GCN, 9866
Bissaldi, E., & Gruber, D. 2009, GCN, 9932
Bissaldi, E., & McBreen, S. 2008, GCN, 8715
Bissaldi, E., & McBreen, S. 2008, GCN, 8750
Bissaldi, E., & McBreen, S. 2008, GCN, 8751
Bissaldi, E., & von Kienlin, A. 2008, GCN, 8433
Bissaldi, E., & von Kienlin, A. 2008, GCN, 8486
Bissaldi, E., & von Kienlin, A. 2008, GCN, 8495
Bissaldi, E., & von Kienlin, A. 2008, GCN, 8622
Bissaldi, E., & von Kienlin, A. 2009, GCN, 8801
Bissaldi, E., & von Kienlin, A. 2009, GCN, 8802
Bissaldi, E., & von Kienlin, A. 2009, GCN, 8803
Bissaldi, E., & von Kienlin, A. 2009, GCN, 8916
Bissaldi, E., & von Kienlin, A. 2009, GCN, 8961
Bissaldi, E., & von Kienlin, A. 2009, GCN, 9865
Bissaldi, E., Briggs, M., Piron, F., Takahashi, H., & Uehara, T. 2009, GCN, 9972
Bissaldi, E., McBreen, S., Connaughton, V., et al. 2008, GCN, 8110
Bissaldi, E., McBreen, S., Connaughton, V., et al. 2008, GCN, 8204
Bissaldi, E., McBreen, S., & von Kienlin, A. 2008, GCN, 8213
Bissaldi, E., McBreen, S., & von Kienlin, A. 2008, GCN, 8214
Bissaldi, E., McBreen, S., Wilson-Hodge, C. A., et al. 2008, GCN, 8263
Bissaldi, E., McBreen, S., & von Kienlin, A. 2008, GCN, 8302
Bissaldi, E., McBreen, S., & Connaughton, V. 2008, GCN, 8369
Briggs, M. S. 2009, GCN, 9059
Briggs, M. S. 2009, GCN, 9299
Briggs, M. S. 2009, GCN, 9301
Briggs, M. S. 2009, GCN, 9302
Briggs, M. S. 2009, GCN, 9957
Briggs, M. S. 2009, GCN, 10164
Briggs, M. S., & van der Horst, A. J. 2008, GCN, 8109
Briggs, M. S., & van der Horst, A. J. 2008, GCN, 8665
Burgess, J. M., & Guiriec, S. 2009, GCN, 10146
Burgess, J. M., Goldstein, A., & van der Horst, A. J. 2009, GCN, 9698
Butler, N. R., Kocevski, D., Bloom, J. S., & Curtis, J. L. 2007, ApJ, 671, 656
Cabrera, J. I., Firmani, C., Avila-Reese, V., et al. 2007, MNRAS, 382, 342
Cenko, S. B., Bloom, J. S., Morgan, A. N., et al. 2009, GCN, 9053
Cenko, S. B., Perley, D. A., & Junkkarinen, V. 2009, GCN, 9518
Chaplin, V. 2009, GCN, 8927
Chaplin, V. 2009, GCN, 9019
Chaplin, V. 2009, GCN, 9346
Chaplin, V. 2009, GCN, 9904
Chaplin, V. 2009, GCN, 10095
Chaplin, V., van der Horst, A. J., & Preece, R. 2008, GCN, 8682
Chornock, R., Perley, D. A., Cenko, S. B., et al. 2009, GCN, 9028
Chornock, R., Perley, D. A., & Cenko, S. B. 2009, 9243
Connaughton V. 2008, GCN, 8498
Connaughton, V. 2008, GCN, 8710
Connaughton, V. 2009, GCN, 8822
Connaughton, V. 2009, GCN, 8821
Connaughton, V. 2009, GCN, 9184
Connaughton, V. 2009, GCN, 9230
Connaughton, V. 2009, GCN, 9399
Connaughton, V. 2009, GCN, 9829
Connaughton, V., & Briggs, M. 2008, GCN, 8408
Connaughton, V., & McBreen, S. 2008, GCN, 8579
Connaughton, V., & van der Horst, A. 2008, GCN, 8206
Cucchiara, A., Fox, D. B., Cenko, S. B., et al. 2008, GCN, 8713
Cucchiara, A., Fox, D. B., & Tanvir, N. 2009, GCN, 9873
Cucchiara, A., Fox, D., Levan, A., et al. 2009, GCN, 10202
Foley, S. 2009, GCN, 10457
Foley, S., & McBreen, S. 2009, GCN, 10449
Fynbo, J. U. 2008, GCN, 8254
Ghirlanda, G., Celotti, A., & Ghisellini, G. 2002, A&A, 393, 409
Ghirlanda, G., Bosnjak, Z., Ghisellini, G., Tavecchio, F., & 2007, MNRAS, 379, 73
Ghirlanda, G., Nava, L., Ghisellini, G., Celotti, A., & Firmani, C. 2009, A&A, 496, 585
Ghirlanda, G., Nava, L., & Ghisellini, G. 2010, A&A, 511, A43
Ghisellini, G., Ghirlanda, G., Nava, L., & Celotti, A. 2010, MNRAS, 144
Goldstein, A. 2009, GCN, 9056
Goldstein, A. 2009, GCN, 9507
Goldstein, A. 2009, GCN, 9508
Goldstein, A. 2009, GCN, 9895
Goldstein, A. 2009, GCN, 10358
Goldstein, A., & Burgess, J. M. 2009, GCN, 9562
Goldstein, A., & Preece, R. 2008, GCN, 8781
Goldstein, A., & Preece, R. 2009, GCN, 8798
Goldstein, A., & van der Horst, A. J. 2009, GCN, 8876
Goldstein, A., & van der Horst, A. J. 2009, GCN, 8963
Goldstein, A., van der Horst, A., & Preece, R. 2008, GCN, 8291
Goldstein, A., Preece, R., & van der Horst, A. J. 2008, GCN, 8793
Goldstein, A., Preece, R. D., & Briggs, M. S. 2010, ApJ, 721, 1329
Greiner, J., Clemens, C., Kruhler, T. et al. 2009, A&A, 498, 89
Gruber, D. 2009, GCN, 10187
Gruber, D. 2009, GCN, 10397
Gruber, D., Bissaldi, E., & McBreen, S. 2009, GCN, 9974
Guidorzi, C., Lacapra, M., Frontera, F., et al. 2010, ArXiv e- prints
Guiriec, S. 2009, GCN, 8897
Guiriec, S. 2009, GCN, 8921
Guiriec, S. 2009, GCN, 9501
Guiriec, S. 2010, GCN, 10372
Guiriec, S. 2010, GCN, 10373
Guiriec, S., & Tierney, D. 2009, GCN, 10406
Guiriec, S., & van der Horst, A. J. 2008, GCN, 8644
Guiriec, S., Connaughton, V., & Briggs, M. 2009, GCN, 9336
Guiriec, S., Briggs, M. S., Connaughton, V., et al. 2010, ApJ, 725, 225
Kaneko, Y., Preece, R. D., Briggs, M. S., et al. 2006, ApJS, 166, 298
Kara, E., Guiriec, S., & Chaplin, V. 2009, GCN, 9692
Kouveliotou, C., & Briggs, M. S. 2008, GCN, 8476
Kouveliotou, C., & Connaughton, V. 2008, GCN, 8784
Kouveliotou, C., & Connaughton, V. 2008, GCN, 8785
Kouveliotou, C., Meegan, C. A., Fishman, G. J., et al. 1993, ApJ, 413, L101
Malesani, D., Goldoni, P., Fynbo, J. P. U., et al. 2009, GCN, 9942
McBreen, S. 2008, GCN, 8533
McBreen, S. 2008, GCN, 8549
McBreen, S. 2009, GCN, 9228
McBreen, S. 2009, GCN, 9310
McBreen, S. 2009, GCN, 9413
McBreen, S. 2009, GCN, 9425
McBreen, S. 2009, GCN, 9535
McBreen, S. 2009, GCN, 9600
McBreen, S. 2009, GCN, 9627
McBreen, S. 2009, GCN, 9631
McBreen, S. 2009, GCN, 9844
McBreen, S. 2009, GCN, 10225
McBreen, S. 2009, GCN, 10266
McBreen, S. 2009, GCN, 10319
McBreen, S., & Bissaldi, E. 2008, GCN, 8775

McBreen, S., & Chaplin, V. 2009, GCN, 10115
McBreen, S., & von Kienlin, A. 2008, GCN, 8680
McBreen, S., von Kienlin A., & Bissaldi, E. 2008, GCN, 8145
McBreen, S., Bissaldi, E., & von Kienlin, A. 2008, GCN, 8167
McBreen, S., Bissaldi, E., & von Kienlin, A. 2008, GCN, 8235
McBreen, S., Connaughton, V., & Wilson-Hodge, C. 2009, GCN, 10226
Meegan, C. 2009, GCN, 9845
Meegan, C. A., & Bhat, P. N. 2009, GCN, 9510
Meegan, C., & van der Horst, A. J. 2009, GCN, 9650
Meegan, C. A., Greiner, J., & Bhat, N. P. 2008, GCN, 8100
Meegan, C., Lichti, G., Bhat, P. N., et al. 2009, ApJ, 702, 791
Nava, L., Ghirlanda, G., Ghisellini, G., & Firmani, C. 2008, MNRAS, 391, 639
Nava, L., Ghirlanda, G., Ghisellini, G., & Celotti, A. 2010, [arXiv:1012.3968]
Omodei, N., Fermi LAT, & Fermi GBM collaborations. 2009, [arXiv:0907.0715]
Paciesas, W. 2009, GCN, 9419
Paciesas, W. 2009, GCN, 9767
Paciesas, W. 2009, GCN, 10345
Paciesas, B., van der Horst, A., & Goldstein, A. 2008, GCN, 8280
Paciesas, B., Briggs, M., & Preece, R. 2008, GCN, 8316
Peer, A., & Ryde, F. 2010, ApJ, submitted, [arXiv:1008.4590]
Preece, R. 2008, GCN, 8678
Preece, R. 2009, GCN, 9130
Preece, R. 2009, GCN, 9131
Preece, R. D., & van der Horst, A. J. 2008, GCN, 8111
Preece, R. D., Briggs, M. S., Mallozzi, R. S., et al. 1998, ApJ, 506, L23
Preece, R. D., Briggs, M. S., Mallozzi, R. S., et al. 2000, ApJS, 126, 19
Prochaska, J. X., Perley, D., & Howard, A. 2008, GCN, 8083
Rau, A. 2009, GCN, 8960
Rau, A. 2009, GCN, 8977
Rau, A. 2009, GCN, 9474
Rau, A. 2009, GCN, 9554
Rau, A. 2009, GCN, 9556
Rau, A. 2009, GCN, 9558
Rau, A. 2009, GCN, 9560
Rau, A. 2009, GCN, 9566
Rau, A. 2009, GCN, 9571
Rau, A. 2009, GCN, 9583
Rau, A. 2009, GCN, 9598
Rau, A. 2009, GCN, 9619
Rau, A. 2009, GCN, 9693
Rau, A. 2009, GCN, 9688
Rau, A. 2009, GCN, 9832
Rau, A. 2009, GCN, 9850
Rau, A. 2009, GCN, 9929
Rau, A. 2009, GCN, 9962
Rau, A. 2009, GCN, 9983
Rau, A. 2009, GCN, 10126
Rau, A., Connaughton, V., & Briggs, M. 2009, GCN, 9057
Rau, A., McBreen, S., & Kruehler, T. 2009, GCN, 9353
Ryde, F. 2005, ApJ, 625, L95
Ryde, F., & Peer, A. 2009, ApJ, 702, 1211
Sakamoto, T., Lamb, D. Q., Kawai, N., et al. 2005, ApJ, 629, 311
Salvaterra, R., Della Valle, M., Campana, S., et al. 2009, Nature, 461, 1258
Tierney, D. 2009, GCN, 10431
Tierney, D., & McBreen, S. 2009, GCN, 10223
van der Horst, A. 2008, GCN, 8141
van der Horst, A. 2008, GCN, 8278
van der Horst, A. J. 2008, GCN, 8329
van der Horst, A. J. 2008, GCN, 8341
van der Horst, A. J. 2008, GCN, 8593
van der Horst, A. J. 2009, GCN, 8805
van der Horst, A. J. 2009, GCN, 8971
van der Horst, A. J. 2009, GCN, 9035
van der Horst, A. J. 2009, GCN, 9300
van der Horst, A. J. 2009, GCN, 9472
van der Horst, A. J. 2009, GCN, 9498
van der Horst, A. J. 2009, GCN, 9661
van der Horst, A. J. 2009, GCN, 9690
van der Horst, A. J. 2009, GCN, 9691
van der Horst, A. J. 2009, GCN, 9760
van der Horst, A. J., & Tierney, D. 2009, GCN, 10539
von Kienlin, A. 2008, GCN, 8374
von Kienlin, A. 2008, GCN, 8505
von Kienlin, A. 2008, GCN, 8521
von Kienlin, A. 2008, GCN, 8586
von Kienlin, A. 2008, GCN, 8640
von Kienlin, A. 2008, GCN, 8824
von Kienlin, A. 2009, GCN, 8853
von Kienlin, A. 2009, GCN, 8877
von Kienlin, A. 2009, GCN, 8902
von Kienlin, A. 2009, GCN, 8912
von Kienlin, A. 2009, GCN, 8918
von Kienlin, A. 2009, GCN, 8922
von Kienlin, A. 2009, GCN, 9040
von Kienlin, A. 2009, GCN, 9055
von Kienlin, A. 2009, GCN, 9229
von Kienlin, A. 2009, GCN, 9271
von Kienlin, A. 2009, GCN, 9392
von Kienlin, A. 2009, GCN, 9412
von Kienlin, A. 2009, GCN, 9424
von Kienlin, A. 2009, GCN, 9447
von Kienlin, A. 2009, GCN, 9579
von Kienlin, A. 2009, GCN, 9662
von Kienlin, A. 2009, GCN, 9792
von Kienlin, A. 2009, GCN, 9804
von Kienlin, A. 2009, GCN, 9812
von Kienlin, A. 2009, GCN, 9813
von Kienlin, A. 2009, GCN, 10210
von Kienlin, A. 2009, GCN, 10381
von Kienlin, A. 2009, GCN, 10546
von Kienlin, A., & Bissaldi, E. 2008, GCN, 8432
von Kienlin, A., & Bissaldi, E. 2008, GCN, 8483
von Kienlin, A., & Bissaldi, E. 2008, GCN, 8496
von Kienlin, A., & Bissaldi, E. 2008, GCN, 8494
von Kienlin, A., McBreen, S., & Bissaldi, E. 2008, GCN, 8107
von Kienlin, A., Bissaldi, E., & McBreen, S. 2008, GCN, 8290
von Kienlin, A., Bissaldi, E., & Gruber, D. 2009, GCN, 10018
von Kienlin, A., Bhat, P. N., & Preece, R. 2009, GCN, 10355
Vreeswijk, P. M., Fynbo, J. P. U., & Malesani, D. 2008, GCN, 8191
Vreeswijk, P., Malesani, D., & Fynbo, J. 2008, GCN, 8301
Wiersema, K., Tanvir, N. R., & Cucchiara, A. 2009, GCN, 10263
Wilson-Hodge, C. A. 2008, GCN, 8144
Wilson-Hodge, C. A. 2008, GCN, 8686
Wilson-Hodge, C. A. 2008, GCN, 8704
Wilson-Hodge, C. A. 2009, GCN, 8972
Wilson-Hodge, C. A. 2009, GCN, 9390
Wilson-Hodge, C. A. 2009, GCN, 9398
Wilson-Hodge, C. A. 2009, GCN, 9713
Wilson-Hodge, C. A. 2009, GCN, 9823
Wilson-Hodge, C. A. 2009, GCN, 9849
Wilson-Hodge, C. A. 2009, GCN, 9856
Wilson-Hodge, C. A. 2009, GCN, 10293
Wilson-Hodge, C. A., & Connaughton, V. 2008, GCN, 8664
Wilson-Hodge, C. A., & Guiriec, S. 2009, GCN, 10448
Wilson-Hodge, C. A., & Preece, R. D. 2009, GCN, 10204
Wilson-Hodge, C. A., & van der Horst, A. J. 2008, GCN, 8116
Xu, D., Fynbo, J. P. U., Tanvir, N., et al. 2009, GCN, 10053

Pages 10 to 25 are available in the electronic edition of the journal at http://www.aanda.org

Table 2. Spectral parameters of the time-averaged spectra of 323 *Fermi*/GBM GRBs fitted with a curved function.

GRB	Δt s	Model	[a]A/10^{-3} ph/cm^2/s	α	E_{peak} keV	β	C-stat	d.o.f.	Fluence/10^{-7} erg/cm^2
080714745	28.672	CPL	8.79± 1.41	–1.14± 0.07	167.7± 16.7	...	765.53	595	73.75± 3.73
080715950	14.336	CPL	7.57± 0.48	–1.27± 0.04	315.5± 38.4	...	784.04	712	59.74± 3.16
080717543	26.624	Band	10.92± 3.55	–0.66± 0.18	119.1± 19.8	–2.11± 0.17	740.76	462	85.89± 19.96
080719529	44.032	CPL	4.67± 2.50	–0.56± 0.30	92.56± 15.0	...	450.01	348	14.87± 1.81
080723557	73.728	Band	34.02± 0.72	–0.85± 0.01	194.0± 3.7	–2.43± 0.05	1281.70	468	1011.00± 32.41
080723913	0.32	CPL	38.28± 14.60	–0.24± 0.30	168.7± 26.3	...	375.81	355	1.66± 0.20
080723985	60.417	CPL	10.18± 0.24	–0.98± 0.02	427.4± 18.7	...	597.02	472	412.89± 9.67
080724401	120.834	Band	9.50± 0.86	–0.97± 0.05	97.96± 4.86	–2.33± 0.09	889.96	591	270.22± 20.53
080725435	37.888	CPL	5.64± 0.29	–1.08± 0.04	322.6± 28.3	...	551.75	474	110.54± 4.93
080725541	0.512	CPL	10.87± 1.25	–0.73± 0.09	1439± 376	...	599.68	594	17.58± 3.38
080727964	81.921	CPL	3.51± 0.18	–1.33± 0.03	314.4± 36.5	...	1166.4	708	164.18± 8.19
080730520	24.576	CPL	9.77± 0.93	–0.84± 0.06	151.9± 8.63	...	714.57	582	47.07± 1.67
080730786	10.24	Band	48.67± 3.72	–0.53± 0.04	113.3± 3.11	–3.05± 0.21	646.78	589	55.54± 2.25
080730786	10.24	CPL	43.41± 2.61	–0.59± 0.04	119.4± 2.53	...	654.99	590	48.98±6.86
080802386	0.384	CPL	24.24± 2.75	–0.73± 0.12	601.4± 124.0	...	401.88	355	9.66± 1.34
080804456	33.792	CPL	3.61± 0.58	–0.99± 0.10	144.0± 15.7	...	642.52	592	26.38± 1.73
080804972	31.744	CPL	9.14± 0.52	–0.72± 0.04	252.7± 13.6	...	757.72	589	98.78± 3.49
080805584	68.609	CPL	4.33± 1.07	–1.02± 0.13	84.23± 8.39	...	567.19	349	37.89± 2.74
080806584	7.168	CPL	32.32± 23.30	–0.23± 0.37	56.85± 5.15	...	350.25	353	4.41± 0.36
080806896	92.162	Band	22.81± 4.98	–0.75± 0.10	49.77± 2.56	–2.27± 0.05	1579.80	703	177.11± 34.11
080807993	27.648	CPL	4.05± 0.25	–1.04± 0.04	883.3± 191.0	...	655.21	586	153.10± 20.19
080808565	25.6	Band	16.70± 2.53	–0.99± 0.07	67.49± 3.44	–2.83± 0.22	554.83	480	49.20± 2.75
080808565	25.6	CPL	14.42± 1.51	–1.06± 0.05	72.12± 2.45	...	558.3	481	42.23±0.89
080808772	178.18	CPL	5.11± 1.21	–0.72± 0.12	62.69± 3.0	...	622.82	476	48.78± 2.32
080809808	34.816	CPL	7.52± 1.73	–1.29± 0.12	62.96± 5.18	...	343.36	240	40.18± 1.95
080810549	81.921	CPL	2.57± 0.09	–1.38± 0.02	944.8± 203.0	...	928.83	599	252.41± 23.76
080812889	30.72	CPL	9.96± 3.06	0.13± 0.24	146.3± 13.10	...	457.14	356	23.30± 1.74
080816503	58.369	Band	13.71± 0.88	–0.92± 0.04	124.3± 5.2	–2.49± 0.13	972.74	595	197.74± 16.32
080816989	3.6	CPL	5.60± 0.23	–0.67± 0.06	1637± 226	...	741.75	599	81.37± 9.02
080817161	91.137	Band	11.43± 0.25	–0.94± 0.02	358.0± 13.5	–2.33± 0.07	825.12	474	906.81± 50.13
080818579	33.793	CPL	2.87± 0.45	–1.33± 0.09	137.2± 21.9	...	530.05	479	29.60± 4.51
080818945	15.36	CPL	5.73± 1.00	–1.45± 0.09	69.36± 6.26	...	506.83	475	19.45± 1.01
080821332	10.24	CPL	16.16± 1.79	–0.97± 0.06	119.10± 7.31	...	388.62	356	28.40± 0.99
080823363	41.984	CPL	3.36± 0.31	–1.31± 0.05	205.2± 26.0	...	778.63	597	57.27± 3.28
080824909	28.672	CPL	5.30± 0.63	–1.12± 0.07	160.9± 17.4	...	555.98	476	42.21± 6.30
080825593	41.984	Band	34.48± 1.13	–0.69± 0.02	189.2± 4.91	–2.34± 0.06	771.61	711	567.08± 28.12
080829790	14.336	Band	71.82± 41.60	–0.10± 0.27	54.69± 5.0	–2.36± 0.11	327.71	356	28.77± 3.58
080831921	81.921	CPL	17.98± 2.70	–0.39± 0.09	89.78± 2.96	...	677.80	475	79.81± 2.29
080904886	25.6	CPL	29.13± 2.98	–1.14± 0.05	39.24± 0.75	...	668.75	587	52.15± 0.95
080905499	0.704	Band	26.28± 9.09	0.66± 0.40	284.6± 47.9	–2.15± 0.17	678.34	594	14.70± 3.24
080905499	0.704	CPL	13.00± 1.65	-0.13± 0.16	515.6± 69.0	...	683.02	595	9.28± 0.92
080905570	38.912	CPL	6.18± 0.98	–1.21± 0.08	84.29± 6.49	...	421.47	357	40.99± 1.69
080906212	7.168	Band	53.09± 4.21	–0.51± 0.05	153.4± 7.26	–2.20± 0.08	649.34	597	120.21± 11.47
080913735	29.696	CPL	8.02± 1.70	–0.70± 0.12	106.6± 8.57	...	376.09	352	25.55± 1.37
080916009	88.581	Band	13.49± 0.23	–1.05± 0.01	515.8± 22.4	–2.16± 0.06	972.11	597	1707.70± 88.50
080916406	60.417	CPL	6.38± 0.59	–0.99± 0.05	123.4± 6.51	...	583.16	482	70.24± 2.12
080920268	43.008	CPL	3.19± 0.80	–0.50± 0.17	162.8± 19.9	...	587.82	478	21.79± 1.76
080924766	41.984	CPL	3.53± 0.47	–1.34± 0.07	109.5± 11.1	...	610.30	600	38.49± 1.81
080925775	35.84	Band	18.65± 0.89	–1.03± 0.03	156.8± 7.07	–2.29± 0.08	807.43	716	278.00± 20.43
080927480	43.008	Band	88.08± 105.00	0.39± 0.53	52.3± 8.36	–1.95± 0.08	522.37	358	101.33± 21.10
081008832	79.873	CPL	2.89± 0.22	–1.15± 0.04	252.7± 26.5	...	878.39	602	98.74± 5.51
081009140	40.96	CPL	51.61± 1.64	–1.66± 0.02	27.22± 0.59	...	463.43	348	419.6± 2.30
081009140	40.96	CPL	54.66± 1.66	–1.64± 0.02	28.11± 0.53	...	607.75	357	419.4± 2.34
081009690	35.84	Band	35.28± 11.50	–0.46± 0.15	69.45± 7.19	–1.88± 0.04	607.21	477	259.21± 7.39
081012045	0.96	CPL	11.35± 1.08	–0.60± 0.10	771.7± 139.0	...	494.99	477	16.92± 2.21
081012549	23.552	CPL	4.82± 0.77	–0.23± 0.15	273.5± 30.6	...	618.62	589	36.15± 3.06
081021398	44.033	CPL	8.44± 1.41	–0.90± 0.10	116.0± 9.44	...	503.39	358	56.53± 2.82
081024851	81.921	Band	15.21± 6.64	–0.83± 0.19	45.38± 4.55	–2.19± 0.06	1037.10	598	123.99± 10.64
081024851	81.921	CPL	4.10± 0.47	–1.33± 0.06	73.8± 3.69	...	1042.0	599	63.64±1.8
081025349	25.6	CPL	7.49± 0.63	–0.53± 0.07	251.8± 16.3	...	859.68	723	59.46± 2.77
081028538	19.456	CPL	18.75± 4.25	–0.70± 0.12	65.02± 3.1	...	560.24	473	19.81± 0.70
081101491	0.704	CPL	12.34± 4.24	–0.34± 0.32	249.0± 54.4	...	510.31	479	2.45± 0.59
081101532	9.725	CPL	23.46± 1.06	–0.70± 0.03	468.7± 20.3	...	604.63	598	172.79± 4.96
081102365	2.5	CPL	6.84± 0.60	–0.73± 0.10	656.3± 131.0	...	592.09	599	19.82± 2.52
081102739	46.081	CPL	9.61± 1.74	–0.55± 0.11	99.37± 5.58	...	623.76	481	35.24± 1.45

Table 2. continued.

GRB	Δt s	Model	[a] A/10^{-3} ph/cm^2/s	α	E_{peak} keV	β	C-stat	d.o.f.	Fluence/10^{-7} erg/cm^2
081107321	3.0	CPL	100.80± 13.60	–0.51± 0.07	70.1± 1.7	...	867.86	717	13.34± 0.26
081109293	36.864	CPL	3.86± 0.36	–1.42± 0.05	200.5± 31.9	...	906.22	710	63.21± 4.43
081110601	20.48	CPL	7.13± 0.37	–1.12± 0.04	361.6± 35.7	...	523.29	478	85.20± 4.30
081115891	0.32	CPL	9.63± 2.57	0.26± 0.45	467.0± 119.0	...	781.88	715	2.90± 0.74
081118876	19.965	Band	68.24± 15.40	–0.46± 0.10	56.79± 2.77	–2.29± 0.05	698.79	601	81.59± 5.19
081121858	26.624	Band	28.77± 3.39	–0.46± 0.08	172.8± 11.5	–2.19± 0.07	411.33	353	284.07± 24.50
081122520	21.504	CPL	12.92± 0.78	–0.83± 0.04	206.5± 10.6	...	761.16	717	78.37± 2.36
081124060	24.576	Band	30.68± 7.82	–1.70± 0.09	10.33± 1.58	–2.71± 0.03	1007.00	718	104.26± 2.95
081125496	10.365	Band	104.00± 6.47	–0.46± 0.04	165.8± 4.69	–2.85± 0.14	667.48	596	213.65± 9.74
081126899	38.912	CPL	5.63± 0.31	–0.97± 0.04	343.6± 29.9	...	595.53	478	116.89± 5.45
081129161	26.749	Band	16.32± 1.33	–0.85± 0.05	202.7± 17.1	–2.08± 0.10	429.12	354	284.24± 34.77
081130629	15.36	CPL	5.15± 0.78	–1.06± 0.09	160.2± 18.8	...	532.57	477	20.54± 1.31
081204004	4.096	CPL	9.74± 2.01	–0.71± 0.14	193.2± 27.4	...	539.29	479	9.48± 0.90
081204517	0.384	CPL	25.79± 6.21	–0.71± 0.17	220.4± 44.0	...	495.78	479	2.79± 0.39
081206275	22.528	CPL	7.48± 0.98	–0.47± 0.10	227.1± 17.8	...	1222.50	477	43.45± 2.48
081207680	103.43	Band	9.37± 0.27	–0.58± 0.02	375.1± 13.2	–2.22± 0.07	1040.40	596	1046.40± 69.28
081209981	0.32	Band	33.19± 2.16	–0.67± 0.07	1057± 192	–2.25± 0.20	478.37	470	39.29± 5.43
081209981	0.32	CPL	35.80± 2.28	–0.714± 0.05	1256± 162	...	482.56	471	30.91± 2.85
081215784	9.468	Band	94.00± 1.29	–0.72± 0.01	417.5± 8.6	–2.32± 0.03	667.83	475	957.61± 22.71
081215880	17.408	Band	15.86± 5.28	–0.40± 0.21	122.2± 14.7	–2.51± 0.28	500.84	482	39.35± 7.83
081215880	17.408	CPL	11.12±2.00	–0.61± 0.13	145.0± 11.0	...	502.95	483	28.65±1.50
081216531	0.768	CPL	34.90± 2.22	–0.75± 0.04	1161.0± 121.0	...	672.08	599	63.26± 4.69
081217983	58.368	CPL	5.66± 0.35	–1.05± 0.04	189.7± 11.2	...	876.48	599	100.14± 3.09
081221681	39.422	Band	71.87± 1.93	–0.82± 0.01	85.86± 0.74	–3.73± 0.20	999.80	600	281.93± 3.35
081221681	39.422	CPL	69.47± 1.65	-0.83±0.01	87.15±0.62	...	1006.1	601	271.8±1.3
081222204	21.504	Band	21.08± 1.15	–0.90± 0.03	167.2± 8.28	–2.33± 0.10	744.67	604	175.58± 16.33
081223419	0.832	CPL	42.27± 4.68	–0.69± 0.08	193.2± 14.1	...	625.15	601	8.27± 0.39
081224887	19.614	CPL	31.30± 0.44	–0.82± 0.01	428.8± 9.48	...	557.12	481	412.31± 5.88
081226044	0.448	CPL	15.05± 2.53	–0.75± 0.18	493.8± 132.0	...	484.56	476	5.42± 0.91
081226156	80.897	CPL	2.09± 0.28	–1.47± 0.07	86.23± 8.05	...	607.11	482	45.46± 2.03
081226509	0.448	CPL	17.53± 2.58	–0.46± 0.16	422.1± 73.4	...	651.05	602	5.26± 0.67
081229187	0.512	CPL	13.04± 2.06	–0.31± 0.20	509.3± 97.8	...	700.39	598	6.24± 0.92
081231140	41.985	CPL	9.82± 0.28	–1.21± 0.02	255.7± 11.0	...	777.75	600	185.35± 3.72
090101758	46.08	CPL	12.6± 0.74	–1.18± 0.03	115.2± 4.67	...	669.54	477	125.8± 2.63
090102122	38.912	CPL	12.35± 0.30	–0.97± 0.01	461.1± 15.3	...	768.50	597	349.15± 6.62
090107681	16.384	CPL	11.76± 3.01	–0.71± 0.16	126.2± 14.5	...	397.43	349	26.18± 1.97
090108020	0.768	CPL	81.89± 9.27	–0.63± 0.07	123.7± 5.75	...	623.92	602	7.58± 0.25
090109332	14.336	CPL	5.05± 1.61	–0.71± 0.20	130.5± 18.9	...	520.62	476	10.29± 0.95
090112332	16.384	CPL	6.05± 0.64	–1.18± 0.07	200.6± 24.6	...	466.31	480	35.38± 2.13
090112729	17.408	CPL	29.30± 1.57	–0.81± 0.03	146.0± 4.49	...	581.79	475	92.42± 1.67
090117632	88.066	CPL	3.02± 0.15	–1.29± 0.03	367.80± 47.2	...	832.40	594	166.12± 9.69
090126227	11.264	CPL	15.62± 4.24	–1.09± 0.12	41.84± 2.14	...	508.89	479	11.80± 0.42
090129880	16.384	CPL	7.34± 0.46	–1.46± 0.04	166.0± 15.1	...	677.97	602	49.01± 2.00
090131090	30.974	Band	81.89± 9.88	–0.87± 0.05	50.66± 1.72	–2.17± 0.02	790.20	596	321.61± 9.91
090202347	18.432	Band	6.65± 0.30	–1.25± 0.03	492.6± 74.9	–2.43± 0.47	763.25	602	126.28± 32.09
090206620	0.384	CPL	25.09± 2.64	–0.58± 0.12	498.5± 75.9	...	509.30	476	8.11± 0.88
090207777	14.336	CPL	4.99± 0.44	–1.22± 0.06	284.0± 40.7	...	911.17	717	35.20± 2.55
090213236	17.408	CPL	2.703± 0.72	–0.38± 0.27	275.9± 52.5	...	750.22	718	15.94 ± 2.26
090217206	34.941	CPL	11.77± 0.21	–0.88± 0.01	573.9± 18.8	...	981.27	718	384.61± 8.04
090222179	26.624	CPL	9.49± 1.37	–0.78± 0.08	107.3± 6.29	...	526.97	477	30.15± 1.13
090227310	16.253	CPL	4.66± 0.16	–0.94± 0.04	1301± 205	...	730.66	604	166.12± 15.52
090227772	0.704	Band	57.06± 0.91	–0.48± 0.02	2013± 77.4	–3.15± 0.20	519.98	477	324.79± 9.85
090228204	0.512	CPL	90.36± 1.72	–0.60± 0.02	885.4± 36.7	...	789.19	725	86.95± 2.66
090228976	9.216	CPL	5.47± 1.08	–0.93± 0.13	159.6± 20.9	...	834.50	724	11.50± 0.82
090301315	13.312	CPL	4.28± 0.44	–1.01± 0.08	349.9± 59.4	...	666.44	601	31.31± 3.06
090305052	3.072	CPL	6.98± 0.38	–0.66± 0.07	899.5± 129.0	...	666.40	602	39.21± 3.99
090306245	16.384	CPL	12.67± 4.97	–0.46± 0.22	76.33± 6.14	...	518.53	481	9.66± 0.59
090308734	1.664	CPL	20.01± 0.71	–0.56± 0.05	631.0± 39.4	...	873.36	842	39.52± 1.70
090310189	94.209	CPL	3.48± 0.35	–1.16± 0.06	193.9± 24.0	...	755.82	477	111.35± 6.97
090319622	67.585	CPL	4.28± 0.33	–1.05± 0.05	202.7± 15.4	...	752.14	480	93.61± 4.17
090320801	53.25	CPL	2.67± 0.95	–1.20± 0.18	68.67± 8.67	...	675.38	476	19.89± 1.87
090323002	197.634	CPL	8.38± 0.08	–1.38± 0.01	719.2± 34.8	...	1861.30	584	1662.40± 35.59
090326633	13.312	CPL	10.96± 2.16	–0.97± 0.11	84.77± 5.87	...	725.87	599	17.21± 0.75
090327404	19.456	CPL	19.06± 2.39	–0.54± 0.08	99.9± 3.64	...	693.48	603	29.31± 0.76
090328401	67.585	CPL	9.22± 0.16	–1.07± 0.01	709.1± 29.5	...	1312.8	718	680.2± 15.55
090328713	0.192	CPL	31.92± 1.39	–0.89± 0.05	1953± 339	...	510.76	473	22.43± 2.95

Table 2. continued.

GRB	Δt s	Model	[a] A/10^{-3} ph/cm^2/s	α	E_{peak} keV	β	C-stat	d.o.f.	Fluence/10^{-7} erg/cm^2
090330279	51.2	CPL	7.95± 0.39	–0.87± 0.03	224.0± 9.68	...	674.70	587	129.90± 3.12
090409288	34.816	CPL	4.15± 1.58	–0.36± 0.28	163.3± 27.4	...	451.95	355	20.38± 2.42
090411838	20.48	CPL	9.86± 0.57	–0.98± 0.04	228.8± 15.1	...	499.66	482	70.58± 2.75
090411991	20.99	Band	13.22± 2.18	–0.81± 0.09	179.0± 27.9	–1.87± 0.10	714.91	355	242.7± 44.06
090413122	22.528	CPL	6.85± 1.11	–0.64± 0.11	174.1± 16.1	...	656.14	595	30.24± 1.74
090419997	52.224	Band	8.06± 1.18	–1.16± 0.07	98.07± 11.5	–2.03± 0.06	1030.00	597	202.91± 19.83
090423330	14.336	CPL	7.19± 2.67	–1.00± 0.20	78.31± 9.98	...	690.83	595	11.67± 1.72
090424592	34.046	Band	53.75± 0.87	–1.02± 0.01	161.9± 2.15	–3.26± 0.18	1179.00	718	501.25± 10.55
090425377	37.89	Band	10.37± 0.84	–1.37± 0.05	110.7± 9.54	–2.32± 0.13	480.57	358	164.95± 40.79
090425377	37.89	CPL	9.06± 0.47	–1.43± 0.03	134.1± 8.04	...	483.37	359	117.6±4.75
090426690	12.288	CPL	4.73± 0.38	–1.27± 0.06	336.4± 60.3	...	668.17	600	33.62± 2.83
090427688	15.36	Band	206.4± 157	0.70± 0.37	58.75± 4.67	-2.36± 0.11	1146	695	27.95± 3.38
090428441	6.144	CPL	27.37± 6.73	–0.55± 0.14	86.14± 5.16	...	670.74	595	10.73± 0.47
090429753	0.832	Band	38.53± 15.60	–0.28± 0.26	178.3± 44.3	–1.65± 0.06	502.93	467	42.34± 7.08
090502777	41.985	CPL	7.11± 1.44	–1.03± 0.14	59.98± 2.79	...	707.05	476	26.49± 1.05
090509215	20.477	CPL	4.21± 0.63	–0.80± 0.11	237.1± 33.2	...	861.94	592	28.22± 2.46
090510016	1.536	Band	31.68± 0.64	–0.82± 0.02	4251± 312	–2.76± 0.25	490.59	479	555.84± 24.03
090510016	1.536	CPL	31.64± 0.90	–0.83± 0.02	4575± 235	...	496.33	480	523.3±21.5
090510325	8.192	CPL	1.28± 0.17	–0.65± 0.13	2522± 594	...	451.84	354	78.72± 15.78
090511684	5.12	CPL	5.50± 0.90	–0.94± 0.11	278.0± 58.3	...	514.72	470	11.88± 1.49
090513916	19.456	CPL	3.66± 0.26	–0.84± 0.08	752.9± 156.0	...	630.28	478	92.38± 13.23
090514726	6.144	CPL	8.75± 1.05	–0.96± 0.09	297.2± 47.0	...	344.75	360	24.51± 2.30
090514734	77.825	CPL	4.30± 0.49	–1.33± 0.06	94.78± 6.4	...	537.21	478	76.40± 2.65
090516137	132.10	CPL	4.74± 0.16	–0.99± 0.02	315.2± 15.3	...	2576.20	717	306.99± 8.19
090516353	136.19	Band	46.04± 19.30	–0.39± 0.17	41.75± 3.04	–2.03± 0.03	599.53	238	92.62± 2.77
090516853	19.456	CPL	4.84± 0.43	–1.45± 0.05	209.6± 37.7	...	560.41	479	44.03± 3.78
090518244	12.29	CPL	16.66± 3.30	–0.60± 0.12	107.9± 7.53	...	370.18	355	19.54± 1.08
090519462	7.168	CPL	7.91± 2.80	–0.64± 0.23	119.5± 15.3	...	814.68	710	6.62± 0.56
090519881	18.432	CPL	2.83± 0.36	–0.55± 0.13	439.1± 79.3	...	824.52	709	36.74± 4.79
090520850	7.168	CPL	17.42± 2.03	–0.64± 0.08	196.4± 15.8	...	555.18	478	28.97± 1.51
090520876	18.432	CPL	39.45± 4.28	–0.93± 0.05	45.06± 0.77	...	585.84	595	37.92± 0.52
090522344	26.624	CPL	6.36± 2.19	–0.89± 0.20	88.33± 9.49	...	672.96	580	18.60± 1.36
090524346	60.417	Band	31.36± 3.77	–0.72± 0.06	71.33± 2.83	–2.21± 0.04	944.97	717	263.23± 13.29
090528173	55.297	Band	37.35± 15.50	–0.75± 0.17	34.64± 2.26	–2.23± 0.03	2375.20	706	116.19± 13.27
090528516	120.83	Band	10.40± 0.32	–1.21± 0.02	181.6± 7.74	–2.31± 0.08	1874.70	721	661.55± 40.19
090529310	6.144	CPL	7.88± 1.26	–0.98± 0.10	164.9± 19.9	...	657.42	599	11.95± 0.80
090529564	12.288	CPL	19.84± 0.87	–1.09± 0.03	244.6± 14.0	...	646.73	592	97.99± 2.83
090530760	172.03	Band	46.21± 2.68	–0.83± 0.03	58.38± 0.94	–2.38± 0.02	2584.20	479	809.44± 14.43
090531775	1.216	CPL	7.69± 0.45	–0.69± 0.08	1729± 333	...	621.25	475	39.35± 5.85
090602564	23.552	CPL	4.52± 0.51	–0.70± 0.11	384.4± 58.2	...	359.26	354	62.13± 6.36
090610723	11.264	CPL	7.92± 2.80	–0.66± 0.22	110.1± 13.8	...	730.68	472	9.49± 0.82
090612619	17.408	CPL	6.16± 0.36	–0.80± 0.05	395.4± 34.8	...	899.22	597	65.29± 3.66
090617208	0.256	Band	39.28± 3.54	–0.37± 0.11	623.5± 99.8	–2.22± 0.24	599.87	600	24.56± 5.37
090617208	0.256	CPL	38.97± 3.72	–0.37± 0.09	652.1± 79.3	...	601.82	601	13.75±1.36
090618353	182.27	Band	41.17± 0.56	–1.33± 0.01	162.6± 2.9	–2.52± 0.04	473.03	232	3381.40± 61.96
090618353	182.27	Band	42.48± 0.59	–1.32± 0.01	156.9± 3.59	–2.51± 0.04	641.11	234	3398.1± 62.00
090620400	17.661	Band	54.70± 2.48	–0.31± 0.03	156.7± 3.5	–2.60± 0.09	750.99	599	179.53± 9.00
090621185	65.537	Band	12.17± 2.07	–1.00± 0.08	63.36± 3.96	–2.41± 0.10	886.34	474	114.05± 9.83
090621417	38.913	CPL	4.00± 0.54	–1.20± 0.08	125.1± 12.2	...	869.21	595	37.43± 1.87
090621922	0.128	CPL	42.44± 6.05	–0.05± 0.22	503.9± 75.4	...	352.39	358	5.42± 0.67
090623107	60.417	CPL	6.25± 0.23	–0.72± 0.03	395.7± 21.2	...	777.00	598	229.37± 8.46
090623913	56.321	CPL	2.44± 0.16	–1.27± 0.05	379.8± 63.8	...	869.79	714	87.09± 7.32
090625234	25.6	CPL	3.08± 0.70	–0.82± 0.15	179.1± 29.1	...	593.40	473	18.61± 1.82
090625560	9.216	CPL	10.26± 1.79	–0.88± 0.12	161.2± 17.7	...	581.70	477	20.64± 1.38
090626189	64.513	Band	30.08± 0.70	–1.17± 0.01	210.7± 6.9	–2.38± 0.05	660.00	467	1057.8± 35.48
090626189	64.513	Band	31.95± 0.77	–1.15± 0.01	194.9± 6.05	–2.34± 0.05	757.78	474	1074.2± 34.82
090630311	6.144	CPL	9.74± 2.04	–1.37± 0.11	61.0± 4.68	...	801.32	696	10.38± 0.45
090704242	86.017	CPL	4.58± 0.32	–1.17± 0.04	241.1± 25.1	...	754.93	355	163.75± 8.00
090706283	195.59	Band	1234±2280	0.37± 0.65	17.4± 0.64	–2.68± 0.06	515.90	235	126.63± 4.39
090708152	14.336	Band	11.14± 7.70	–0.80± 0.31	51.14± 7.9	–2.58± 0.32	642.32	597	10.86± 2.15
090708152	14.336	CPL	6.58± 2.54	–1.03±0.18	59.57±5.35	...	643.44	598	8.38±0.50
090709630	18.432	CPL	6.86± 0.93	–0.96± 0.08	137.5± 12.5	...	700.37	600	25.12± 1.33
090711850	88.065	CPL	3.25± 0.26	–1.04± 0.06	298.3± 36.1	...	1050.90	470	135.22± 8.46
090712160	63.489	CPL	2.09± 0.18	–0.78± 0.07	432.8± 58.3	...	617.35	479	90.30± 7.62
090713020	49.153	Band	68.23± 11.10	0.32± 0.09	85.97± 2.27	–2.84± 0.12	3295.50	704	86.28± 4.08
090717034	68.61	Band	22.80± 1.08	–0.93± 0.03	114.9± 3.31	–2.30± 0.05	1232.10	819	431.96± 20.58

Table 2. continued.

GRB	Δt s	Model	[a] A/10^{-3} ph/cm^2/s	α	E_{peak} keV	β	C-stat	d.o.f.	Fluence/10^{-7} erg/cm^2
090717111	0.384	CPL	9.90± 1.21	–0.19± 0.22	695.8± 132.0	...	680.84	708	6.50± 0.96
090718762	30.717	Band	26.46± 0.81	–1.15± 0.02	164.1± 5.1	–2.81± 0.19	820.15	589	277.44± 15.05
090719063	19.71	Band	77.07± 1.53	–0.66± 0.01	228.8± 3.78	–3.14± 0.14	708.11	471	497.53± 12.02
090719063	19.71	CPL	73.70±1.24	–0.68± 0.01	239.7± 3.28	...	716.72	472	452.7±3.75
090720276	6.144	CPL	49.05± 6.40	–0.66± 0.08	108.0± 5.01	...	382.60	353	31.12± 0.98
090720710	17.022	CPL	6.67± 0.26	–1.00± 0.03	792.5± 92.3	...	626.43	588	142.45± 9.88
090725838	19.456	Band	67.07± 62.40	–0.21± 0.40	45.19± 6.26	–2.21± 0.10	447.58	346	39.65± 6.35
090725838	19.456	CPL	7.80± 1.63	–1.15±0.11	81.61± 7.16	...	454.82	347	23.27±1.19
090730608	19.46	CPL	11.74± 2.01	–0.45± 0.11	130.5± 8.49	...	806.54	704	24.56± 1.24
090802235	0.128	CPL	113.50± 12.60	–0.61± 0.10	337.6± 37.0	...	342.61	355	7.05± 0.54
090802666	38.913	Band	7.59± 6.40	–1.09± 0.36	38.68± 6.81	–2.42± 0.19	396.41	351	29.68± 5.05
090804940	11.264	CPL	138.40± 5.40	–0.59± 0.02	97.15± 1.07	...	477.88	466	125.71± 0.95
090805622	59.393	Band	15.33± 11.70	–0.80± 0.34	51.46± 9.55	–2.16± 0.09	767.95	355	105.19± 19.14
090807832	6.144	Band	117.00± 148.00	–0.49± 0.49	27.36± 2.86	–2.47± 0.10	791.60	704	11.21± 0.83
090809978	19.456	Band	36.32± 1.43	–0.84± 0.02	199.5± 7.82	–2.29± 0.08	615.21	474	338.76± 25.30
090810659	112.64	Band	24.30± 18.30	–0.72± 0.30	38.96± 6.36	–1.95± 0.04	1737.50	351	336.09± 28.15
090810781	36.864	Band	60.06± 28.90	–0.21± 0.22	48.56± 3.41	–2.37± 0.08	668.28	474	58.96± 9.06
090811696	16.384	CPL	1.89± 0.22	–1.17± 0.09	778.2± 296.0	...	1631.3	580	35.29± 6.56
090813174	9.725	CPL	8.74± 0.73	–1.50± 0.05	128.6± 12.7	...	571.21	464	30.96± 1.26
090814368	0.576	CPL	13.50± 1.07	–0.57± 0.10	742.4± 125.0	...	812.85	715	11.62± 1.50
090814950	173.06	CPL	1.60± 0.05	–1.26± 0.03	1679± 474	...	684.56	348	544.44± 95.10
090815300	39.936	CPL	11.04± 4.48	0.02± 0.27	103.1± 8.28	...	508.08	358	18.08± 1.24
090815438	24.576	Band	35.93± 11.20	–1.03± 0.13	32.36± 1.43	–2.72± 0.11	657.34	473	50.59± 2.39
090815946	60.416	CPL	3.26± 0.43	–1.04± 0.08	156.1± 17.7	...	1466.90	586	48.93± 3.14
090819607	0.448	CPL	10.41± 1.53	–0.60± 0.19	544.5± 132.0	...	707.48	711	4.42± 0.72
090820027	32.77	Band	167.30± 1.90	–0.67± 0.01	205.2± 1.83	–2.81± 0.04	550.05	344	1716.50± 22.27
090820509	12.288	CPL	6.69± 1.84	–1.48± 0.13	32.94± 2.93	...	452.79	467	11.30± 0.44
090824918	56.321	CPL	19.08± 6.73	–0.90± 0.16	30.33± 1.3	...	720.02	450	31.23± 0.96
090826068	17.408	CPL	6.80± 2.35	–0.31± 0.23	126.6± 14.1	...	667.63	590	10.41± 0.85
090828099	86.017	Band	7.60± 0.42	–1.24± 0.03	171.2± 12.9	–2.40± 0.17	440.05	354	310.24± 37.88
090829672	93.186	Band	20.08± 0.28	–1.48± 0.01	194.7± 5.86	–2.39± 0.07	1808.90	807	1161.80± 51.27
090829702	32.768	CPL	10.96± 1.69	–0.58± 0.10	124.9± 7.5	...	560.51	465	41.51± 1.67
090831317	48.719	CPL	5.74± 0.24	–1.52± 0.03	260.2± 28.6	...	407.13	353	158.98± 6.83
090902401	2.048	CPL	13.28± 1.54	0.00± 0.18	419.6± 42.4	...	543.13	472	19.17± 1.66
090902462	30.207	CPL	78.07± 0.71	–0.63± 0.01	716.3± 6.07	...	1003.10	579	3223.60± 28.46
090904058	70.657	CPL	11.01± 0.65	–1.29± 0.03	123.2± 5.91	...	338.52	232	208.29± 4.39
090904581	51.201	CPL	1.68± 0.23	–0.58± 0.15	434.3± 82.8	...	1168.80	710	59.38± 9.73
090907017	39.936	CPL	5.34± 0.67	–0.36± 0.11	248.3± 21.3	...	403.26	352	60.34± 3.87
090907808	1.024	CPL	23.82± 1.79	–0.16± 0.10	403.8± 28.5	...	768.32	714	15.62± 0.87
090908314	65.537	CPL	2.56± 0.57	–1.27± 0.11	71.0± 6.27	...	697.46	467	27.55± 1.58
090908341	23.677	CPL	3.03± 0.28	–0.61± 0.09	656.6± 107.0	...	529.10	471	88.18± 10.18
090909487	26.624	CPL	9.53± 2.41	–1.20± 0.15	96.36± 11.1	...	556.83	463	48.23± 3.47
090910812	54.273	Band	10.41± 0.66	–0.78± 0.05	246.0± 17.3	–2.35± 0.14	588.76	470	313.98± 35.81
090910812	54.273	CPL	9.48± 0.38	–0.84± 0.03	282.7±12.6	...	594.47	471	211.5±5.97
090912660	77.825	Band	22.11± 6.03	–0.30± 0.14	69.8± 3.83	–2.71± 0.18	1383.30	463	73.93± 6.46
090912660	77.825	CPL	15.87± 2.57	–0.46± 0.09	76.53± 2.47	...	1389.5	464	57.16± 1.40
090915650	12.288	CPL	6.04± 0.66	–0.76± 0.09	283.3± 32.9	...	611.91	590	29.71± 2.21
090917661	30.72	CPL	2.56± 0.50	–0.82± 0.16	275.3± 56.2	...	848.71	590	31.07± 3.69
090920035	44.032	Band	6.23± 2.14	–1.24± 0.18	89.49± 20.6	–2.16± 0.14	1219.60	470	104.15± 30.20
090922539	24.576	Band	19.53± 1.09	–0.95± 0.03	149.0± 6.7	–2.51± 0.15	1215.00	813	146.66± 11.55
090922605	36.864	CPL	4.21± 0.36	–0.97± 0.10	463.3± 70.6	...	439.68	348	113.36± 11.38
090924625	0.192	CPL	24.80± 2.63	–0.55± 0.12	697.1± 138.0	...	489.05	471	6.56± 1.00
090925389	29.696	Band	13.58± 2.03	–0.75± 0.09	154.2± 16.5	–2.11± 0.12	382.37	347	175.71± 27.93
090926181	19.709	Band	165.0± 1.22	–0.71± 0.005	289.9± 2.26	–2.55± 0.02	1762.3	828	1860.3± 18.55
090926181	19.709	Band	164.2± 1.21	–0.71± 0.005	291.8± 2.28	–2.55± 0.02	1514.4	816	1859.1± 18.52
090926914	65.537	CPL	33.24± 3.18	–0.19± 0.06	94.49± 1.9	...	934.85	472	98.12± 1.59
090928646	18.432	CPL	7.49± 1.46	–0.56± 0.15	191.4± 21.8	...	506.35	468	29.22± 1.84
090929190	13.312	CPL	10.66± 0.53	–0.62± 0.06	483.9± 36.9	...	663.10	581	113.68± 5.46
091003191	23.552	CPL	18.54± 0.49	–0.99± 0.02	410.2± 17.2	...	492.87	353	281.12± 6.12
091005679	16.384	CPL	4.14± 0.69	–0.89± 0.12	206.6± 30.5	...	667.09	596	20.03± 1.80
091010113	9.216	CPL	46.96± 1.76	–1.10± 0.02	144.1± 4.05	...	441.23	357	105.67± 1.58
091012783	0.832	CPL	36.09± 1.84	–0.46± 0.07	684.9± 59.2	...	397.71	356	42.52± 2.62
091017985	44.033	Band	32.09± 46.30	–0.13± 0.62	43.38± 8.06	–2.23± 0.13	757.32	592	33.32± 6.60
091017985	44.033	CPL	3.51± 1.11	–1.11± 0.17	73.37± 7.75	...	761.42	593	19.5± 1.28
091018957	0.32	CPL	28.29± 7.13	–0.53± 0.26	298.7± 61.6	...	497.34	474	3.62± 0.48
091020900	28.672	Band	7.87± 0.81	–1.20± 0.06	186.8± 24.8	–2.29± 0.18	417.10	354	123.78± 18.06

Table 2. continued.

GRB	Δt s	Model	[a] A/10^{-3} ph/cm^2/s	α	E_{peak} keV	β	C-stat	d.o.f.	Fluence/10^{-7} erg/cm^2
091020977	49.153	CPL	3.52± 0.11	–1.08± 0.03	851.8± 102.0	...	925.83	713	223.95± 16.22
091024372	98.305	CPL	3.26± 0.18	–1.04± 0.04	452.3± 56.4	...	558.58	465	228.29± 16.71
091024380	195.59	Band	5.01± 0.27	–1.01± 0.03	189.4± 12.1	–2.17± 0.10	1793.30	468	559.25± 60.64
091030613	34.816	CPL	10.06± 1.05	–0.71± 0.07	139.8± 6.64	...	687.16	595	54.34± 1.57
091030828	41.086	Band	11.62± 0.44	–0.80± 0.03	382.2± 22.2	–2.27± 0.09	587.67	466	481.68± 38.63
091031500	43.01	CPL	6.12± 0.16	–0.96± 0.03	584.5± 36.5	...	1237.80	830	245.52± 9.46
091101143	16.384	CPL	24.97± 1.81	–0.88± 0.04	131.3± 5.52	...	382.14	353	70.31± 1.64
091103912	25.60	CPL	7.28± 0.60	–1.05± 0.05	213.9± 19.1	...	518.98	473	63.89± 2.82
091107635	11.264	CPL	4.28± 1.14	–1.10± 0.15	132.0± 23.1	...	714.10	592	10.76± 1.10
091109895	24.577	CPL	7.16± 1.91	–0.98± 0.14	69.69± 5.28	...	560.31	476	16.87± 0.84
091112737	40.961	CPL	3.36± 0.17	–1.08± 0.04	618.1± 97.1	...	609.67	478	131.66± 11.42
091112928	29.696	CPL	4.58± 0.41	–1.05± 0.06	249.2± 31.2	...	907.50	717	54.18± 3.94
091115177	67.585	CPL	1.46± 0.12	–0.98± 0.07	590.8± 135.0	...	788.69	600	92.65± 14.07
091117080	98.306	CPL	3.76± 0.70	–1.13± 0.10	99.44± 9.64	...	872.56	357	65.20± 3.57
091120191	59.393	Band	19.95± 0.65	–1.12± 0.02	130.2± 3.37	–2.96± 0.25	1234.30	591	305.72± 14.26
091120191	59.393	CPL	19.26± 0.53	–1.14± 0.02	135.1± 2.65	...	1238.6	592	274.4± 2.73
091123298	367.17	CPL	4.46± 0.21	–1.27± 0.03	124.7± 4.86	...	1459.70	352	427.61± 10.97
091126333	0.384	CPL	23.79± 3.46	–0.51± 0.16	401.4± 66.9	...	491.06	480	5.66± 0.64
091126389	0.032	CPL	61.79± 9.66	–0.20± 0.17	616.4± 97.4	...	616.74	715	2.71± 0.35
091127976	13.054	Band	116.50± 14.60	–1.25± 0.05	34.25± 1.02	–2.22± 0.01	617.97	466	247.74± 5.35
091128285	138.243	CPL	9.71± 0.35	–1.09± 0.02	182.8± 7.14	...	897.54	352	406.12± 8.16
091201089	38.913	CPL	3.65± 1.44	–0.99± 0.20	67.75± 7.64	...	730.75	478	13.48± 1.00
091202072	23.552	CPL	3.10± 0.86	–1.26± 0.15	85.77± 11.6	...	699.74	596	13.84± 1.04
091202219	129.03	Band	15.37± 8.74	–0.73± 0.23	36.64± 3.23	–2.38± 0.08	1298.40	468	91.63± 18.06
091207333	27.648	CPL	8.86± 0.91	–0.71± 0.07	162.6± 9.69	...	947.13	716	46.46± 1.69
091208410	13.312	CPL	17.21± 1.34	–1.29± 0.04	118.9± 7.5	...	411.99	348	59.77± 1.73
091209001	52.225	CPL	67.14± 14.30	–0.14± 0.11	59.74± 1.67	...	788.59	237	62.35± 1.58
091220442	25.6	CPL	8.25± 0.68	–1.21± 0.04	119.6± 6.39	...	937.93	594	49.71± 1.36
091221870	39.937	Band	13.82± 1.12	–0.57± 0.05	194.9± 11.6	–2.22± 0.10	673.54	466	244.89± 27.57
091223191	0.64	CPL	14.35± 2.93	–0.06± 0.25	359.0± 60.0	...	673.18	598	4.73± 0.64
091223511	65.537	CPL	8.99± 1.06	–0.34± 0.08	157.5± 7.19	...	1761.70	710	76.97± 2.42
091227294	35.84	CPL	5.75± 0.40	–1.00± 0.05	252.4± 21.8	...	536.96	475	80.67± 3.88
091230260	11.264	CPL	5.41± 2.39	–0.09± 0.37	168.± 26.3	...	622.45	597	7.32± 0.90
091230712	23.552	CPL	9.60± 2.86	–0.61± 0.18	107.8± 11.5	...	478.34	353	21.89± 1.64
091231206	60.417	CPL	13.72± 1.18	–0.50± 0.06	139.2± 4.82	...	749.85	591	103.08± 2.54
100116897	47.105	CPL	8.98± 0.15	–1.06± 0.01	929.3± 59.9	...	652.06	470	600.49± 22.15
100117879	0.256	CPL	41.98± 9.66	–0.15± 0.21	285.5± 43.6	...	499.96	476	3.63± 0.44
100118100	7.168	CPL	4.04± 0.41	–0.35± 0.15	717.8± 138.0	...	456.70	471	47.20± 6.67
100122616	30.721	Band	52.51± 7.50	–1.03± 0.06	44.88± 1.58	–2.36± 0.04	582.56	465	178.80± 6.15
100130729	74.754	CPL	6.25± 0.45	–1.09± 0.04	135.4± 6.91	...	814.27	590	105.50± 2.84
100130777	91.137	CPL	3.86± 0.24	–1.18± 0.04	218.4± 17.3	...	816.36	466	135.10± 5.21
100131730	11.645	CPL	25.43± 1.38	–0.97± 0.03	151.5± 5.74	...	462.53	464	66.18± 1.28
100201588	140.29	CPL	3.97± 0.28	–1.30± 0.04	105.6± 4.82	...	1457.60	697	132.66± 2.95
100204024	83.97	CPL	6.15± 0.38	–0.89± 0.04	180.0± 8.38	...	1268.70	698	129.89± 3.53
100204566	52.225	CPL	3.31± 0.50	–1.42± 0.08	117.9± 17.1	...	442.10	353	53.61± 3.56
100204858	0.32	CPL	18.55± 7.23	0.59± 0.60	312.3± 59.8	...	352.37	351	2.19± 0.39
100205490	17.408	CPL	16.11± 5.64	0.03± 0.23	112.8± 9.22	...	394.40	354	13.76± 0.95
100206563	0.256	CPL	46.48± 3.60	–0.37± 0.09	502.8± 48.9	...	540.24	479	10.71± 0.78
100207665	28.672	CPL	3.05± 0.66	–0.51± 0.21	303.1± 58.5	...	263.37	236	35.61± 5.11
100208386	0.32	CPL	7.53± 0.89	–0.66± 0.15	1829± 650	...	490.43	473	11.49± 3.20
100210101	25.6	CPL	4.27± 0.89	–1.26± 0.11	90.66± 10.0	...	965.81	828	21.75± 1.59
100211440	33.792	CPL	27.44± 1.89	–0.91± 0.04	113.0± 3.51	...	421.00	350	139.34± 2.47
100212550	8.192	CPL	12.67± 1.48	0.41± 0.15	278.6± 15.3	...	486.65	474	29.48± 1.48
100212588	2.56	CPL	7.35± 2.96	–1.02± 0.23	102.0± 18.2	...	646.21	592	2.93± 0.36
100216422	0.32	CPL	13.91± 2.33	–0.03± 0.25	471.5± 82.4	...	642.13	595	3.93± 0.70
100218194	40.961	CPL	5.21± 1.21	–0.24± 0.17	148.8± 12.3	...	892.26	590	23.18± 1.31
100219026	58.37	CPL	2.61± 0.17	–1.05± 0.06	678.9± 145.0	...	479.70	358	160.70± 20.78
100221368	25.60	Band	18.99± 11.30	–0.16± 0.31	77.39± 10.4	–2.31± 0.18	543.54	478	30.02± 2.32
100221368	25.60	CPL	8.16± 2.01	–0.57± 0.15	101.6± 7.61	...	547.0	479	17.78± 0.99
100223110	0.384	CPL	21.19± 1.19	–0.34± 0.09	1082± 126	...	457.11	477	26.40± 2.57
100224112	53.249	CPL	4.91± 0.39	–1.32± 0.05	162.6± 15.0	...	628.69	357	90.03± 3.73
100225115	27.648	CPL	4.46± 0.26	–0.69± 0.06	411.4± 34.7	...	846.28	720	78.74± 4.42
100225580	13.312	CPL	12.41± 0.58	–1.00± 0.03	283.0± 18.2	...	776.90	602	72.80± 2.60
100225703	16.384	CPL	3.67± 0.41	–0.47± 0.11	437.9± 57.8	...	830.68	704	42.64± 4.10
100228544	43.009	CPL	3.21± 0.90	–0.97± 0.15	93.4± 10.9	...	594.28	472	18.14± 1.59
100301068	0.192	CPL	25.54± 5.10	–0.56± 0.20	423.5± 101.0	...	333.75	356	3.28± 0.45

Table 2. continued.

GRB	Δt s	Model	[a] A/10^{-3} ph/cm^2/s	α	E_{peak} keV	β	C-stat	d.o.f.	Fluence/10^{-7} erg/cm^2
100301223	36.865	CPL	11.96± 2.29	–0.52± 0.12	109.8± 6.71	...	413.72	350	38.93± 1.66
100304004	73.729	CPL	4.21± 0.23	–1.26± 0.05	493.8 ± 72.7	...	549.55	352	240.5± 18.22
100304534	21.504	CPL	5.48± 0.71	–1.27± 0.08	183.7± 32.1	...	484.80	355	42.38± 3.10
100307928	21.504	Band	62.62± 73.70	–0.32± 0.47	32.53± 4.16	–2.35± 0.11	575.10	470	22.46± 3.01
100311518	13.312	CPL	6.96± 0.99	–0.32± 0.14	316.9± 39.0	...	556.83	469	38.86± 3.46
100313288	19.456	CPL	11.04± 0.96	–0.59± 0.06	208.3± 12.6	...	523.12	480	52.17± 2.24
100318611	21.504	CPL	14.43± 5.81	–0.90± 0.20	46.29± 2.91	...	564.56	472	15.62± 0.80
100322045	41.985	Band	32.22± 0.68	–0.83± 0.01	271.7± 6.79	–2.21± 0.04	704.36	475	990.42± 34.85
100323542	38.913	CPL	3.51± 0.49	–0.98± 0.09	221.4± 34.2	...	466.56	351	46.14± 3.89
100324172	21.118	CPL	33.36± 0.57	–0.59± 0.01	430.0± 9.85	...	550.40	474	479.92± 7.18
100325246	19.456	CPL	4.71± 1.81	–1.37± 0.18	45.12± 4.86	...	406.04	356	12.35± 8.20
100325275	9.216	CPL	20.98± 2.55	–0.47± 0.08	168.3± 10.4	...	487.46	475	31.31± 1.38
100326294	0.8	CPL	8.39±1.27	0.10± 0.28	670.8 ± 129	...	348.21	353	16.13± 2.8
100326402	125.95	CPL	4.17± 0.25	–1.06± 0.04	212.1± 14.0	...	595.57	473	179.98± 5.92
100328141	0.768	CPL	16.70± 1.24	–0.64± 0.07	986.9± 162.0	...	695.79	593	27.00± 3.46
100330309	22.528	Band	18.54± 3.69	–0.76± 0.10	88.73± 7.14	–2.29± 0.11	712.09	586	71.03± 7.66
100330309	22.528	CPL	10.03± 1.00	–0.98± 0.08	115.1± 5.56	...	717.35	587	38.22± 1.04

Notes. [(a)] For all models the pivot energy for the amplitude is 100 keV. Fluences are in the range 8 keV–35 MeV.

Table 3. Spectral parameters of the time-averaged spectra of 109 *Fermi*/GBM GRBs fitted with a power law.

GRB	Δt s	Model	[a]A/10^{-3} ph/cm^2/s	α	C–stat	d.o.f.	Fluence/10^{-7} erg/cm^2
080714086	7.17	PL	1.41± 0.11	–1.36± 0.04	522.07	475	10.45± 1.98
080714425	41.98	PL	0.97± 0.06	–1.70± 0.05	338.38	352	33.09± 6.62
080723339	...	...	...	...	...	...	...
080803772	121.86	PL	1.12± 0.03	–1.73± 0.02	605.62	356	115.4± 9.54
080805496	38.91	PL	0.89± 0.05	–2.14± 0.04	583.33	474	27.55± 2.32
080808451	23.55	PL	1.02± 0.09	–1.69± 0.06	539.85	470	19.73± 8.46
080815917	1.09	PL	6.69± 0.37	–1.48± 0.04	474.87	359	6.80± 0.49
080817720	7.17	PL	1.69± 0.18	–1.15± 0.04	441.30	480	15.96± 26.59
080822647	1.50	PL	1.13± 0.21	–1.52± 0.15	657.48	600	1.54± 1.08
080828189	8.19	PL	1.07± 0.10	–1.55± 0.08	475.22	357	7.79± 2.56
080830368	52.22	PL	2.07± 0.06	–1.49± 0.02	581.27	479	100.7± 7.38
080831053	0.05	PL	12.87± 2.56	–1.29± 0.12	383.43	474	0.72± 0.26
080905705	52.22	PL	0.92± 0.03	–1.68± 0.03	786.31	481	39.52± 4.95
080912360	19.46	PL	1.42± 0.10	–1.76± 0.03	672.00	588	22.00± 8.47
080919790	0.19	PL	6.64± 0.69	–1.48± 0.08	456.65	480	1.20± 0.17
080928628	33.79	PL	0.93± 0.05	–2.00± 0.04	827.24	724	24.44± 1.19
081003644	69.63	PL	2.50± 0.06	–1.59± 0.02	613.20	359	150.0± 12.66
081006604	32.77	PL	0.66± 0.06	–1.51± 0.06	350.86	360	19..76± 5.40
081006872	20.48	PL	0.54± 0.06	–1.57± 0.10	516.86	479	9.66± 3.93
081007224	13.31	PL	1.69± 0.15	–2.19± 0.06	269.01	235	18.39± 2.22
081017474	26.62	PL	0.79± 0.08	–2.12± 0.05	412.03	361	16.74± 38.55
081022364	15.36	PL	1.42± 0.07	–1.64± 0.04	480.84	474	18.32± 3.73
081024245	0.13	PL	21.34± 3.13	–1.36± 0.07	455.35	474	2.84± 0.26
081024891	0.90	PL	4.79± 0.29	–1.32± 0.04	504.06	478	4.65± 0.26
081101167	10.24	PL	0.16± 0.09	–1.16± 0.11	331.17	259	2.08± 1.24
081105614	0.26	PL	7.33± 1.52	–1.19± 0.06	665.64	601	2.34± 0.45
081113230	0.51	PL	13.25± 0.62	–1.45± 0.04	531.88	484	6.52± 0.54
081119184	0.35	PL	6.26± 0.53	–1.37± 0.05	407.51	362	2.25± 0.46
081120618	29.70	PL	0.63± 0.05	–2.36± 0.03	841.60	480	16.88± 3.09
081122614	0.06	PL	28.24± 1.60	–1.56± 0.05	434.28	484	1.59± 0.16
081130212	44.00	PL	1.33± 0.20	–2.08± 0.10	295.46	241	45.77± 5.60
081206604	5.60	PL	1.66± 0.12	–1.76± 0.06	504.47	481	7.41± 1.25
081206987	12.29	PL	1.75± 0.07	–1.41± 0.03	545.82	479	21.34± 2.08
081213173	0.26	PL	5.14± 0.55	–1.39± 0.07	475.67	485	1.33± 0.32
081225257	79.87	PL	1.16± 0.03	–1.61± 0.02	1465.2	604	79.06± 6.86
081229675	0.30	PL	8.55± 0.68	–1.41± 0.05	390.70	363	2.54± 0.53
081230871	1.02	PL	1.69± 0.46	–1.12± 0.05	623.48	593	2.36± 0.53
090108322	0.19	PL	13.56± 0.71	–1.33± 0.04	659.19	603	2.78± 0.40
090113778	12.29	PL	1.94± 0.07	–1.67± 0.03	596.61	601	19.74± 2.43
090117335	25.60	PL	0.97± 0.07	–1.76± 0.06	616.39	482	19.81± 4.80
090117640	12.29	PL	1.87± 0.09	–2.24± 0.03	507.16	483	19.23± 1.13
090120627	13.31	PL	0.75± 0.08	–1.27± 0.05	605.85	480	11.37± 0.95
090126245	10.00	PL	0.58± 0.08	–1.38± 0.09	709.11	595	5.96± 2.32
090219074	0.06	PL	24.22± 2.70	–1.36± 0.06	464.93	473	1.61± 0.37
090225009	5.12	PL	1.25± 0.18	–1.30± 0.07	293.69	229	7.07± 0.87
090303542	0.19	PL	5.07± 0.85	–2.02± 0.12	539.85	475	0.75± 0.13
090304216	4.10	PL	2.66± 0.13	–1.44± 0.04	672.79	598	10.52± 1.82
090307167	14.34	PL	1.68± 0.11	–1.65± 0.05	422.78	349	20.09± 4.98
090309767	45.06	PL	1.60± 0.04	–1.81± 0.02	693.93	596	56.35± 3.87
090316311	2.24	PL	4.66± 0.24	–1.61± 0.04	507.71	480	8.90± 1.64
090320045	6.14	PL	1.43± 0.09	–1.44± 0.05	600.32	592	8.48± 1.84
090320418	6.14	PL	1.77± 0.10	–1.50± 0.04	619.24	603	10.01± 1.96
090331681	1.22	PL	3.83± 0.26	–1.30± 0.04	521.77	480	5.17± 0.77
090403314	17.41	PL	1.55± 0.06	–1.60± 0.03	661.80	483	23.25± 3.40
090405663	0.45	PL	6.87± 0.44	–1.41± 0.05	684.17	600	3.06± 0.66
090412061	0.26	PL	7.43± 0.71	–1.29± 0.06	330.03	359	2.13± 0.45
090418816	0.90	PL	4.05± 0.32	–1.40± 0.05	537.02	484	3.64± 0.74
090422150	12.29	PL	0.80± 0.13	–1.97± 0.11	464.02	347	7.61± 1.28
090426066	7.17	PL	1.17± 0.09	–1.65± 0.06	702.59	715	6.98± 1.95
090427644	9.22	PL	0.86± 0.08	–1.39± 0.07	664.58	599	7.99± 2.22
090428552	34.82	PL	2.46± 0.07	–1.97± 0.02	421.37	359	66.11± 4.28
090429530	20.48	PL	1.96± 0.07	–1.50± 0.02	579.58	471	37.01± 3.66
090513941	17.42	PL	1.67± 0.10	–1.63± 0.05	534.89	476	24.52± 4.96
090514006	50.18	PL	1.91± 0.05	–1.90± 0.02	511.98	479	74.16± 2.03
090518080	6.14	PL	2.24± 0.15	–1.70± 0.05	325.49	355	11.20± 2.30

Table 3. continued.

GRB	Δt s	Model	[a]A/10^{-3} ph/cm^2/s	α	C–stat	d.o.f.	Fluence/10^{-7} erg/cm^2
090520832	1.80	PL	2.20± 0.30	–1.73± 0.11	394.51	352	3.19± 1.34
090606471	15.36	PL	1.91± 0.14	–1.57± 0.06	256.26	224	25.60± 2.34
090608052	21.50	PL	1.29± 0.06	–1.83± 0.04	576.90	478	21.64± 3.00
090610648	5.12	PL	2.59± 0.11	–1.33± 0.03	638.70	595	14.27± 0.57
090610883	12.29	PL	1.70± 0.11	–1.69± 0.05	373.80	359	17.16± 3.75
090616157	6.14	PL	1.10± 0.10	–1.41± 0.06	625.31	595	6.71± 0.68
090620901	1.50	PL	3.85± 0.23	–1.34± 0.04	629.31	601	6.14± 0.95
090621447	23.55	PL	1.52± 0.06	–1.70± 0.03	827.86	701	29.14± 1.37
090626707	...	...	...	...	...	...	...
090629543	24.58	PL	0.95± 0.08	–1.42± 0.05	429.22	351	23.09± 1.84
090701225	12.29	PL	1.29± 0.09	–1.86± 0.05	488.67	481	12.26± 1.02
090703329	10.24	PL	1.81± 0.08	–1.74± 0.04	629.50	604	14.83± 2.11
090704783	28.67	PL	1.37± 0.05	–1.77± 0.03	724.17	724	31.25± 3.73
090718720	5.12	PL	1.83± 0.13	–1.44± 0.05	844.33	834	9.09± 0.62
090726218	...	...	...	...	...	...	...
090817036	38.01	PL	1.73± 0.06	–1.69± 0.03	537.07	356	53.63± 6.45
090823133	14.34	PL	1.31± 0.07	–1.86± 0.04	891.83	584	14.53± 2.12
090909854	0.51	PL	5.85± 0.37	–1.45± 0.05	764.56	705	2.88± 0.61
090927422	1.34	PL	5.03± 0.34	–1.64± 0.06	434.54	355	5.69± 1.35
091002685	3.07	PL	1.09± 0.10	–1.67± 0.08	467.41	472	2.76± 0.88
091006360	...	...	...	...	...	...	...
091015129	9.22	PL	1.54± 0.24	–1.94± 0.13	309.51	236	10.91± 4.24
091017861	7.17	PL	1.48± 0.12	–1.79± 0.06	486.83	471	8.38± 1.54
091019750	0.32	PL	4.52± 0.44	–1.33± 0.06	625.12	591	1.56± 0.17
091023021	11.26	PL	1.25± 0.11	–1.87± 0.07	586.49	480	10.94± 2.66
091026485	9.22	PL	1.83± 0.11	–1.63± 0.05	410.53	357	14.28± 3.28
091026550	19.46	PL	2.31± 0.14	–1.59± 0.04	333.53	238	38.80± 2.57
091102607	9.22	PL	2.72± 0.11	–1.44± 0.02	589.53	472	24.25± 2.56
091106762	23.55	PL	1.83± 0.09	–1.63± 0.04	311.74	235	36.41± 5.35
091122163	11.26	PL	0.57± 0.07	–1.58± 0.10	488.69	471	5.62± 2.50
091123081	17.41	PL	1.60± 0.09	–1.74± 0.04	404.44	352	22.40± 4.07
091207888	...	...	...	...	...	...	...
091215234	9.22	PL	1.78± 0.11	–1.76± 0.05	491.14	479	13.07± 2.11
091219462	12.29	PL	1.53± 0.08	–1.70± 0.04	637.67	595	15.26± 2.48
091224373	0.32	PL	5.12± 0.67	–1.25± 0.06	385.30	358	1.91± 0.43
091231540	21.50	PL	1.01± 0.08	–1.89± 0.06	570.20	479	16.83± 1.41
100101028	0.77	PL	3.66± 0.31	–1.39± 0.06	772.56	712	2.85± 0.73
100101988	10.24	PL	0.71± 0.08	–1.23± 0.05	831.18	597	8.68± 1.56
100107074	0.20	PL	10.38± 0.90	–1.34± 0.05	647.36	597	2.20± 0.41
100111176	19.46	PL	1.21± 0.06	–1.72± 0.04	675.60	597	19.06± 3.16
100112418	56.32	PL	0.08± 0.01	–3.52± 0.07	2685.5	700	22.92± 11.84
100126460	16.38	PL	0.75± 0.08	–1.39± 0.06	364.49	359	12.40± 3.24
100207721	93.19	PL	0.20± 0.01	–3.98± 0.01	1377.0	592	218.3± 1.88
100225249	13.31	PL	1.26± 0.20	–1.35± 0.07	349.10	356	17.73± 4.63
100228873	6.14	PL	1.92± 0.13	–1.77± 0.05	473.53	478	9.35± 0.79
100306199	11.26	PL	0.82± 0.09	–1.58± 0.09	426.76	354	8.02± 1.12
100313509	55.30	PL	0.99± 0.04	–1.89± 0.03	587.85	470	42.35± 4.62
100315361	25.60	PL	0.98± 0.05	–1.40± 0.04	498.38	477	25.27± 3.77
100327405	...	...	...	...	...	...	...
100330856	15.36	PL	0.90± 0.08	–1.65± 0.07	344.77	356.00	11.53± 3.68

Notes. The fluence is computed in the 8 keV–1 MeV energy range. The 6 GRBs for which the analysis cannot be performed (lack of data) are also listed. [a]The pivot energy for the amplitude is 100 keV.

Table 4. Spectral parameters of the peak spectra of 235 *Fermi*/GBM GRBs fitted with a curved function.

GRB	Δt s	t_1 s	t_2 s	Model	[a] A/10^{-3} ph/cm^2/s	α	$E_{\rm peak}$ keV	β	C–stat	d.o.f.	Flux/10^{-7} erg/cm^2/s
080714745	28.672	2.56	3.58	Band	752.90±712.00	0.72± 0.51	78.5± 10.5	–2.07± 0.08	669.28	598	24.01± 3.80
080715950	14.336	1.02	2.05	CPL	21.67± 1.15	–1.22± 0.04	569.1± 90.2	...	788.22	717	18.81± 1.50
080723557	73.7288	55.04	56.06	CPL	115.00± 3.05	–0.65± 0.03	407.3± 12.9	...	522.12	472	72.47± 1.60
080723985	60.417	13.06	14.08	CPL	36.28± 1.87	–0.79± 0.05	460.2± 35.8	...	523.09	475	26.58± 1.30
080724401	120.834	21.12	22.14	Band	132.70± 23.80	–0.41± 0.10	109.1± 7.12	–2.43± 0.12	661.31	595	17.25± 1.80
080725435	37.888	6.14	7.17	CPL	13.40± 1.77	–0.87± 0.11	330.3± 56.2	...	501.36	477	6.67± 0.70
080727964	81.921	14.34	15.36	CPL	20.01± 2.84	–0.55± 0.13	286.1± 36.0	...	947.11	829	7.54± 0.67
080730520	24.576	3.84	4.86	CPL	34.86± 6.16	–0.78± 0.12	148.6± 14.2	...	756.82	699	6.26± 0.38
080730786	10.24	1.28	2.30	Band	111.80± 9.49	–0.39± 0.06	154.8± 5.84	–3.31± 0.31	637.68	593	16.61± 0.72
080802386	0.384	–0.06	0.00	CPL	23.52± 3.84	–0.13± 0.24	1051.0± 238.0	...	345.89	355	90.87± 18.02
080804972	31.744	7.17	8.19	CPL	13.63± 1.77	–0.88± 0.10	351.1± 67.4	...	677.90	593	7.30± 0.88
080806584	7.168	–1.02	0.00	CPL	440.90±397.00	1.05± 0.54	71.05± 4.95	...	369.70	353	1.72± 0.14
080806896	92.162	27.65	28.67	CPL	56.14± 8.02	–0.76± 0.08	117.2± 7.52	...	876.70	823	7.28± 0.30
080807993	27.648	0.00	1.70	CPL	16.22± 0.73	–0.84± 0.05	1141.0± 205.0	...	598.22	590	34.17± 4.60
080808565	25.6	5.12	6.14	CPL	49.46± 12.40	–0.85± 0.13	71.97± 4.69	...	525.41	481	3.98± 0.18
080808772	178.178	–43.01	–38.91	CPL	50.63± 39.40	0.02± 0.41	59.62± 5.34	...	532.08	479	0.68± 0.06
080816503	58.369	35.33	36.35	CPL	52.22± 6.37	–0.72± 0.08	140.8± 8.69	...	629.35	600	8.24± 0.33
080816989	3.6	0.00	1.00	CPL	10.96± 0.49	–0.36± 0.05	1755.0± 141.0	...	678.95	599	76.55± 5.50
080817161	91.137	7.17	8.19	Band	55.48± 3.41	–0.72± 0.05	351.3± 30.2	–2.11± 0.09	526.58	477	62.71± 6.41
080818579	33.793	0.00	1.41	CPL	19.34± 3.02	–0.75± 0.12	217.7± 27.7	...	550.70	479	5.52± 0.87
080818945	15.36	2.82	3.84	CPL	18.85± 9.15	–1.16± 0.25	56.75± 7.33	...	555.73	475	2.05± 0.18
080821332	10.24	0.00	1.28	CPL	56.98± 6.17	–0.63± 0.07	150.2± 8.1	...	365.48	358	9.00± 0.34
080824909	28.672	0.00	1.28	CPL	29.94± 3.43	–0.96± 0.07	200.3± 21.6	...	527.57	479	8.97± 0.55
080825593	41.984	2.69	3.71	Band	174.20± 10.50	–0.42± 0.04	217.4± 9.56	–2.32± 0.07	731.22	716	75.76± 5.20
080831921	81.921	2.05	3.07	CPL	84.61± 40.60	0.46± 0.38	122.6± 10.5	...	542.29	478	3.15± 0.26
080904886	25.6	6.14	7.17	CPL	111.40± 15.80	–1.05± 0.07	52.79± 1.58	...	651.02	588	8.89± 0.20
080905499	0.704	–0.06	0.00	CPL	26.57± 5.69	–0.06± 0.30	532.3± 103.0	...	521.99	595	29.45± 4.70
080906212	7.168	0.00	1.66	Band	157.80± 10.50	–0.33± 0.04	173.3± 6.47	–2.44± 0.11	645.18	597	40.15± 3.10
080913735	29.696	17.66	18.69	CPL	88.48± 40.90	0.34± 0.31	111.5± 9.69	...	395.09	352	2.96± 0.24
080916009	88.581	4.61	5.63	CPL	30.34± 0.63	–1.07± 0.02	2073.0± 253.0	...	635.98	602	91.06± 7.70
080916406	60.417	2.56	3.58	CPL	46.85± 9.57	–0.11± 0.15	154.0± 10.7	...	490.80	485	4.87± 0.27
080925775	35.84	5.38	6.40	Band	104.80± 9.68	–0.65± 0.06	165.0± 10.1	–2.43± 0.13	748.54	721	30.45± 3.00
081008832	79.8727	15.36	16.38	CPL	19.88± 5.48	–0.36± 0.20	176.4± 23.9	...	638.80	605	3.21± 0.33
081009140	40.9606	2.82	3.84	CPL	781.70± 45.20	–1.07± 0.03	53.63± 0.62	...	543.60	465	66.85± 0.62
081009690	35.84	1.41	2.43	Band	61.61± 27.80	–0.37± 0.25	117.7± 23.1	–1.93± 0.11	459.41	480	20.58± 1.22
081012045	0.96	0.38	0.45	CPL	18.20± 2.60	–0.49± 0.21	1089.00± 364.0	...	474.78	480	51.06± 12.99
081021398	44.0326	2.32	3.34	CPL	84.63± 35.70	0.34± 0.32	131.7± 12.2	...	391.66	359	4.21± 0.35
081025349	25.6	1.54	2.56	CPL	18.73± 3.10	–0.16± 0.18	307.3± 36.5	...	700.06	723	7.25± 0.69
081028538	19.456	0.00	2.05	Band	373.60±269.00	0.36± 0.34	59.66± 5.91	–2.25± 0.10	580.83	472	7.04± 0.65
081101532	9.725	1.54	2.56	Band	37.49± 2.71	–0.48± 0.08	476.0± 50.3	–2.23± 0.16	613.62	601	57.45± 8.69
081102365	2.5	0.00	0.50	CPL	16.85± 3.36	–0.43± 0.19	322.2± 58.8	...	682.00	599	7.40± 0.96
081102739	46.081	18.43	19.46	CPL	26.93± 14.10	–0.64± 0.29	83.19± 11.8	...	557.64	481	1.87± 0.19
081107321	3.0	1.00	1.50	CPL	322.60± 65.80	–0.07± 0.12	76.87± 2.35	...	777.73	722	8.37± 0.23
081110601	20.48	0.00	0.83	CPL	49.78± 1.44	–0.82± 0.03	715.9± 46.4	...	500.38	481	61.64± 2.60
081118876	19.965	7.68	8.70	CPL	71.44± 10.90	–0.68± 0.09	98.99± 5.01	...	667.64	605	6.73± 0.23
081121858	26.624	6.14	7.17	Band	59.89± 21.60	–0.21± 0.28	206.9± 43.8	–1.86± 0.09	331.23	353	51.68± 8.31
081122520	21.504	0.00	2.05	Band	66.42± 4.98	–0.44± 0.06	205.1± 10.0	–2.60± 0.16	726.41	721	20.66± 1.80
081124060	24.576	11.78	12.80	Band	92.83± 30.30	–1.53± 0.13	18.31± 1.89	–3.05± 0.17	774.02	718	9.96± 0.51
081125496	10.365	2.18	3.20	Band	272.40± 21.40	–0.01± 0.06	198.2± 6.81	–2.96± 0.20	634.47	600	54.25± 3.20
081126899	38.912	2.18	3.20	Band	30.35± 3.96	–0.55± 0.10	296.2± 41.9	–2.19± 0.22	474.14	480	24.82± 6.20
081129161	26.749	0.00	1.15	Band	89.76± 10.80	–0.27± 0.09	234.1± 19.8	–2.13± 0.09	361.41	356	54.37± 6.59
081130629	15.36	2.30	3.33	CPL	16.67± 3.38	–0.97± 0.13	165.1± 25.1	...	436.86	479	4.07± 0.35
081204004	4.096	0.00	1.02	CPL	18.39± 4.27	–0.69± 0.16	191.5± 31.1	...	578.38	482	4.26± 0.46
081204517	0.384	–0.06	0.00	CPL	58.32± 13.00	–0.38± 0.20	344.0± 72.0	...	487.69	479	28.25± 5.12
081207680	103.426	37.89	38.91	CPL	11.01± 0.55	–0.87± 0.06	1375.0± 275.0	...	632.02	601	27.74± 4.10
081209981	0.32	0.00	0.06	CPL	77.05± 5.17	–0.23± 0.10	829.6± 84.1	...	461.40	474	175.67± 14.88
081215784	9.468	1.28	2.30	Band	223.10± 3.11	–0.53± 0.01	623.0± 15.0	–2.32± 0.03	530.58	478	440.12± 10.99
081216531	0.768	0.58	0.64	CPL	102.80± 4.50	–0.38± 0.06	1408.0± 120.0	...	639.76	603	487.21± 36.02
081217983	58.368	8.19	9.22	CPL	55.18± 8.03	–0.31± 0.10	157.1± 9.2	...	599.19	603	7.00± 0.30
081221681	39.422	20.99	22.02	Band	399.40± 28.90	–0.16± 0.04	109.8± 2.08	–4.05± 0.40	690.01	604	24.15± 0.50
081222204	21.504	3.33	4.35	CPL	54.67± 4.42	–0.88± 0.04	225.0± 12.6	...	622.31	605	17.59± 0.58
081223419	0.832	0.06	0.13	CPL	107.50± 24.50	–0.49± 0.17	194.1± 23.8	...	555.39	601	22.06± 1.89
081224887	19.614	2.21	3.23	CPL	106.00± 2.85	–0.40± 0.03	423.8± 12.0	...	538.23	481	71.94± 1.50
081226156	80.897	6.66	7.68	CPL	29.73± 9.81	–0.78± 0.18	84.82± 8.02	...	508.15	482	2.61± 0.17
081226509	0.448	0.00	0.06	CPL	58.75± 13.80	0.24± 0.30	336.2± 49.3	...	631.12	602	26.32± 3.30

Table 4. continued.

GRB	Δt s	t_1 s	t_2 s	Model	[a] A/10^{-3} ph/cm^2/s	α	$E_{\rm peak}$ keV	β	C–stat	d.o.f.	Flux/10^{-7} erg/cm^2/s
081231140	41.985	25.60	26.62	CPL	47.49± 2.91	–0.86± 0.05	256.9± 15.5	...	619.12	600	17.64± 0.60
090101758	46.08	92.67	93.70	CPL	68.09± 7.31	–0.71± 0.07	160.5± 9.72	...	527.43	480	12.68± 0.48
090102122	38.912	15.62	16.64	CPL	49.02± 2.17	–0.25± 0.05	389.9± 15.7	...	585.22	600	29.28± 0.91
090108020	0.768	0.00	0.06	CPL	369.60± 68.60	–0.15± 0.13	134.3± 7.62	...	556.86	602	30.65± 1.50
090112729	17.408	2.56	3.58	CPL	81.09± 6.68	–0.62± 0.06	181.6± 8.26	...	574.59	477	16.59± 0.49
090113778	12.288	0.00	1.02	CPL	19.07± 3.58	–0.63± 0.14	211.0± 27.5	...	597.50	600	4.83± 0.39
090126227	11.264	–0.51	0.00	CPL	96.54± 70.20	–0.49± 0.34	46.53± 4.32	...	532.10	479	2.12± 0.17
090129880	16.384	0.77	1.79	CPL	17.35± 1.43	–1.24± 0.06	381.1± 71.4	...	608.98	603	10.95± 0.98
090131090	30.974	6.40	7.42	Band	3976±988.00	0.13± 0.11	40.78± 0.91	–2.75± 0.04	752.99	600	27.47± 0.56
090202347	18.432	8.70	9.73	CPL	22.58± 1.90	–0.93± 0.07	333.0± 39.4	...	589.33	603	11.52± 0.84
090206620	0.384	0.00	0.06	CPL	42.90± 5.81	–0.17± 0.21	580.1± 98.9	...	478.73	476	53.22± 7.30
090207777	14.336	0.00	2.05	CPL	11.08± 1.26	–0.64± 0.12	373.1± 50.0	...	790.65	717	6.20± 0.58
090217206	34.941	6.27	7.30	CPL	33.15± 1.14	–0.66± 0.04	636.1± 41.5	...	821.85	722	38.06± 1.70
090222179	26.624	4.10	5.12	CPL	29.67± 8.93	–0.37± 0.20	138.5± 15.6	...	554.69	477	3.24± 0.27
090227310	16.253	1.92	2.94	CPL	10.68± 0.66	–0.81± 0.08	1270.0± 301.0	...	642.72	604	26.25± 3.88
090227772	0.704	0.00	0.06	Band	217.70± 6.01	–0.06± 0.03	2011.0± 64.1	–3.56± 0.22	478.55	477	3451± 96.56
090228204	0.512	0.00	0.06	Band	376.50± 8.87	–0.21± 0.03	870.4± 34.4	–3.42± 0.31	790.15	724	1051± 41.97
090228976	9.216	0.00	1.66	CPL	6.58± 1.63	–0.33± 0.28	315.5± 61.3	...	822.25	724	2.74± 0.35
090305052	3.072	0.00	0.48	CPL	15.41± 0.92	–0.49± 0.09	1028.0± 148.0	...	729.87	602	39.72± 4.50
090308734	1.664	0.64	0.70	CPL	39.67± 4.80	–0.26± 0.14	689.2± 92.5	...	782.96	842	63.69± 6.47
090310189	94.209	0.00	0.90	CPL	29.22± 6.97	–0.11± 0.22	237.6± 31.8	...	510.51	480	6.88± 0.75
090323002	197.634	65.54	66.56	CPL	45.55± 1.76	–0.69± 0.04	461.9± 26.7	...	578.70	588	33.89± 1.30
090326633	13.312	6.14	7.17	CPL	90.72± 51.30	–0.31± 0.30	57.89± 4.29	...	780.11	719	2.06± 0.14
090327404	19.456	9.22	10.24	CPL	27.48± 10.40	–0.69± 0.21	87.39± 9.33	...	645.55	603	2.22± 0.16
090328401	67.585	23.55	24.58	CPL	61.99± 1.78	–0.76± 0.03	458.8± 19.8	...	950.01	843	45.36± 1.30
090328713	0.192	0.00	0.06	CPL	54.01± 2.88	–0.87± 0.06	1782.0± 338.0	...	508.36	473	183.30± 25.95
090330279	51.2	12.29	13.31	CPL	20.32± 1.92	–0.88± 0.08	331.5± 41.2	...	640.04	591	10.18± 0.83
090411838	20.48	10.24	11.26	CPL	22.87± 3.19	–0.70± 0.10	247.4± 31.6	...	461.88	482	7.49± 0.69
090411991	20.989	5.63	6.66	CPL	16.44± 2.57	–0.92± 0.12	318.3± 65.3	...	435.50	358	7.97± 1.04
090413122	22.528	5.12	6.14	CPL	16.66± 3.60	–0.68± 0.17	205.0± 29.6	...	621.81	599	4.20± 0.39
090423330	14.336	–4.10	0.00	CPL	64.94± 36.50	–0.09± 0.31	68.22± 5.34	...	637.81	599	1.36± 0.09
090424592	34.046	0.00	1.28	Band	437.70± 9.65	–0.83± 0.01	152.0± 2.01	–3.50± 0.18	845.42	723	91.15± 1.40
090425377	37.8887	58.56	59.58	CPL	28.98± 2.35	–1.36± 0.05	250.8± 37.6	...	594.02	596	14.21± 0.92
090428441	6.144	0.00	1.60	CPL	66.37± 15.50	–0.43± 0.14	92.03± 5.1	...	632.45	595	3.97± 0.17
090502777	41.9845	37.50	38.53	CPL	49.58± 15.40	–0.64± 0.18	84.5± 6.46	...	517.73	479	3.52± 0.20
090510016	1.536	0.51	0.58	CPL	98.84± 3.49	–0.70± 0.03	2618.0± 219.0	...	435.31	480	698.93± 46.26
090511684	5.12	0.00	2.05	CPL	12.17± 2.77	–0.60± 0.16	200.1± 30.7	...	472.78	470	2.82± 0.30
090514006	50.177	0.00	1.54	CPL	18.35± 1.45	–0.97± 0.06	419.1± 63.0	...	553.29	478	12.06± 1.10
090514726	6.144	0.00	0.38	CPL	50.60± 8.62	–0.35± 0.16	265.7± 30.5	...	356.74	360	15.94± 1.32
090516137	132.098	80.90	81.92	CPL	11.67± 1.56	–0.86± 0.11	369.1± 71.5	...	799.94	722	6.59± 0.78
090516853	19.456	0.00	1.95	CPL	20.12± 1.52	–1.09± 0.05	351.8± 49.1	...	464.90	479	11.34± 1.03
090518080	6.144	0.00	1.28	CPL	12.76± 2.36	–1.02± 0.12	191.7± 32.6	...	743.42	718	3.81± 0.35
090518244	12.288	0.00	1.15	CPL	56.33± 11.50	–0.19± 0.15	152.4± 11.2	...	384.28	355	6.14± 0.41
090519462	7.168	–1.54	0.00	CPL	20.62± 6.87	–0.58± 0.22	120.5± 13.8	...	749.59	710	2.25± 0.17
090520850	7.168	2.18	3.20	CPL	29.25± 5.08	–0.58± 0.13	212.6± 26.0	...	512.26	481	7.30± 0.57
090520876	18.432	3.07	4.10	CPL	109.30± 29.10	–0.70± 0.13	49.66± 1.88	...	617.29	594	4.09± 0.24
090522344	26.624	0.00	2.05	CPL	14.12± 4.36	–0.92± 0.19	119.8± 16.9	...	603.96	580	2.31± 0.19
090524346	60.417	5.12	6.14	Band	120.80± 12.80	–0.46± 0.07	140.2± 6.69	–3.07± 0.35	693.96	717	17.15± 1.30
090528173	55.297	3.07	4.10	Band	20.64± 16.40	–1.31± 0.35	46.47± 13.1	–2.30± 0.20	778.25	711	4.39± 0.93
090528516	120.834	9.22	10.24	Band	47.67± 4.20	–0.84± 0.06	262.6± 29.2	–2.19± 0.16	720.24	721	34.61± 5.53
090529310	6.144	0.00	1.28	CPL	21.30± 5.93	–0.65± 0.18	128.2± 14.6	...	716.78	599	2.74± 0.21
090529564	12.288	9.02	10.05	CPL	117.80± 5.68	–0.75± 0.03	199.9± 6.74	...	770.20	714	30.06± 0.63
090530760	172.032	4.10	5.12	Band	265.40± 75.50	0.48± 0.18	122.1± 8.25	–2.31± 0.11	564.01	479	21.43± 2.70
090602564	23.552	2.82	3.84	CPL	9.12± 1.68	–0.28± 0.27	552.8± 145.0	...	359.99	354	9.94± 2.10
090612619	17.408	0.00	2.05	Band	24.27± 1.64	–0.47± 0.07	427.0± 40.6	–2.21± 0.18	735.93	596	32.46± 5.80
090617208	0.256	0.00	0.06	Band	66.88± 9.77	0.74± 0.29	520.9± 73.2	–2.23± 0.20	590.25	600	228.68± 46.95
090618353	182.275	64.00	65.03	Band	244.90± 9.05	–0.91± 0.03	313.2± 14.0	–2.42± 0.07	244.46	233	173.00± 7.30
090620400	17.661	4.35	5.38	Band	159.50± 10.50	0.03± 0.05	207.1± 6.61	–2.96± 0.22	706.78	599	34.05± 2.30
090621185	65.537	9.22	10.24	CPL	35.27± 13.60	–0.67± 0.21	84.22± 9.03	...	478.60	475	2.62± 0.19
090621417	38.913	4.10	5.12	CPL	28.89± 7.51	–0.40± 0.19	157.2± 17.2	...	701.48	595	3.98± 0.31
090621922	0.128	0.00	0.06	CPL	51.30± 11.70	–0.30± 0.27	405.4± 90.3	...	325.22	358	32.66± 5.80
090623107	60.417	0.00	1.15	CPL	24.25± 1.52	–0.18± 0.08	509.9± 39.5	...	605.09	598	23.68± 1.60
090623913	56.321	2.05	3.07	CPL	11.35± 1.16	–1.04± 0.09	518.3± 126.0	...	753.31	714	9.24± 1.30
090626189	64.513	2.82	3.84	Band	421.50± 49.70	–0.22± 0.07	133.9± 6.21	–2.30± 0.06	508.49	467	75.07± 3.90
090630311	6.144	0.00	2.05	CPL	28.38± 6.27	–1.09± 0.12	64.76± 3.94	...	709.68	696	3.08± 0.12
090709630	18.432	2.05	3.07	CPL	24.96± 6.77	–0.65± 0.17	128.7± 16.1	...	647.26	600	3.26± 0.27

Table 4. continued.

GRB	Δt s	t_1 s	t_2 s	Model	[a] A/10^{-3} ph/cm^2/s	α	$E_{\rm peak}$ keV	β	C–stat	d.o.f.	Flux/10^{-7} erg/cm^2/s
090711850	88.065	0.51	1.54	CPL	29.30± 7.05	–0.13± 0.21	205.6± 23.0	...	497.66	473	5.31± 0.50
090713020	49.153	3.07	4.10	Band	330.90±243.00	1.42± 0.51	103.1± 8.44	–2.95± 0.40	755.81	709	3.76± 0.67
090717034	68.609	4.86	5.89	Band	70.84± 6.24	–0.88± 0.05	176.1± 14.2	–2.17± 0.10	876.79	825	35.05± 4.20
090718762	30.717	21.50	22.53	Band	160.30± 7.76	–0.75± 0.03	198.9± 7.79	–2.63± 0.14	630.16	593	54.72± 3.60
090719063	19.709	4.35	5.38	Band	230.30± 8.17	–0.30± 0.03	275.2± 7.18	–3.01± 0.16	499.00	473	91.51± 3.60
090720276	6.144	0.00	1.22	CPL	105.10± 16.30	–0.49± 0.10	123.5± 6.86	...	396.80	354	10.77± 0.43
090720710	17.022	5.76	6.78	CPL	30.50± 1.16	–0.84± 0.04	657.8± 57.4	...	652.62	592	33.79± 2.00
090730608	19.456	3.20	4.22	CPL	18.32± 3.56	–0.68± 0.15	219.0± 32.9	...	813.71	704	5.03± 0.58
090802235	0.128	0.00	0.06	CPL	177.40± 22.90	–0.55± 0.11	306.8± 33.7	...	305.28	355	74.18± 5.70
090804940	11.264	1.47	2.50	CPL	414.10± 25.60	–0.35± 0.04	114.1± 1.99	...	478.08	466	32.00± 0.41
090807832	6.144	0.00	1.86	CPL	22.19± 6.04	–1.42± 0.13	35.04± 2.7	...	779.06	705	2.72± 0.10
090809978	19.456	3.07	4.10	Band	157.30± 12.90	–0.47± 0.05	193.4± 11.2	–2.16± 0.07	471.81	477	72.31± 6.00
090810659	112.642	109.57	110.59	CPL	38.87± 15.70	–1.27± 0.19	43.15± 4.11	...	417.79	352	4.09± 0.25
090810781	36.864	5.12	6.14	CPL	26.98± 12.40	–0.68± 0.26	89.25± 11.5	...	486.29	475	2.20± 0.21
090811696	16.384	–0.26	0.00	CPL	8.32± 1.06	–0.42± 0.22	999.8± 287.0	...	735.55	701	21.86± 6.60
090813174	9.725	0.00	1.54	Band	66.11± 9.69	–0.71± 0.08	140.6± 13.0	–2.21± 0.10	495.58	463	21.35± 2.80
090814368	0.576	0.13	0.19	CPL	32.77± 3.37	–0.39± 0.15	837.5± 170.0	...	703.23	715	66.80± 11.00
090814950	173.058	67.58	68.61	CPL	11.47± 1.54	–0.68± 0.14	618.9± 169.0	...	354.62	348	12.60± 2.74
090815438	24.576	16.38	17.41	CPL	70.14± 13.20	–1.16± 0.09	55.58± 2.73	...	535.53	476	7.43± 0.24
090819607	0.448	–0.06	0.00	CPL	51.19± 13.40	0.30± 0.36	313.9± 44.6	...	637.90	711	19.56± 2.40
090820027	32.769	33.79	34.82	Band	741.90± 18.70	–0.48± 0.02	240.5± 4.65	–2.80± 0.06	418.86	344	269.83± 5.70
090820509	12.2882	0.00	0.90	CPL	46.15± 13.80	–0.81± 0.16	71.03± 5.09	...	512.15	467	3.40± 0.17
090824918	56.321	5.12	6.14	CPL	61.48± 61.50	–0.84± 0.45	30.42± 3.6	...	480.41	450	1.54± 0.13
090826068	17.408	7.17	8.19	CPL	13.29± 3.62	–0.86± 0.18	169.2± 32.6	...	634.31	590	3.02± 0.35
090828099	86.017	52.22	53.25	CPL	42.57± 2.92	–1.16± 0.05	258.5± 25.0	...	405.22	355	18.77± 0.94
090829672	93.186	46.08	47.10	Band	157.80± 5.64	–1.06± 0.02	225.3± 10.8	–2.28± 0.07	965.85	813	95.14± 6.19
090829702	32.768	4.61	5.63	CPL	23.99± 7.56	–0.12± 0.27	199.4± 27.8	...	490.97	465	4.09± 0.44
090831317	48.719	8.78	9.81	CPL	23.67± 2.30	–1.15± 0.07	300.1± 46.5	...	396.34	353	11.81± 0.95
090902401	2.048	0.00	0.51	CPL	23.34± 3.72	0.20± 0.24	396.1± 49.6	...	475.60	472	15.02± 1.60
090902462	30.207	8.70	9.73	CPL	63.11± 3.32	0.08± 0.06	971.6± 19.6	...	600.95	583	257.73± 4.25
090904058	70.657	21.50	22.53	CPL	23.63± 3.36	–1.24± 0.10	196.7± 28.5	...	211.88	233	8.70± 0.63
090904581	51.201	1.54	2.56	CPL	6.34± 1.50	0.81± 0.55	450.6± 81.7	...	710.85	710	6.48± 1.27
090908341	65.537	6.27	7.30	CPL	5.59± 0.88	–0.06± 0.29	657.1± 150.0	...	531.71	474	9.34± 1.80
090910812	54.2731	18.43	19.46	CPL	19.60± 2.46	–0.60± 0.13	363.7± 49.4	...	488.82	471	10.54± 0.99
090915650	12.288	0.00	1.54	CPL	7.91± 1.22	–0.59± 0.17	449.0± 98.7	...	592.15	590	5.72± 0.89
090917661	30.72	0.00	1.28	CPL	15.19± 4.03	–0.64± 0.21	191.7± 30.3	...	700.66	594	3.40± 0.35
090920035	44.032	–8.19	–4.10	CPL	13.04± 4.14	–1.26± 0.18	81.61± 11.6	...	550.39	471	2.38± 0.21
090922539	24.576	2.05	3.07	CPL	70.94± 4.10	–0.73± 0.04	196.8± 7.66	...	845.97	820	17.51± 0.44
090922605	36.864	0.53	2.26	CPL	12.30± 1.11	–0.18± 0.19	654.1± 74.2	...	316.45	348	18.92± 1.93
090924625	0.192	0.00	0.06	CPL	34.09± 5.37	–0.27± 0.21	607.9± 131.0	...	455.30	471	43.96± 7.80
090926181	19.709	3.33	4.35	Band	448.30± 8.37	–0.37± 0.01	280.3± 4.31	–2.43± 0.03	966.09	833	255.22± 5.00
090926914	65.537	18.94	19.97	CPL	42.23± 10.20	–0.59± 0.15	120.9± 11.0	...	464.77	472	4.73± 0.28
090928646	18.432	0.00	1.79	CPL	28.73± 3.76	–0.35± 0.13	214.1± 12.6	...	562.83	471	6.31± 0.30
090929190	13.312	0.00	1.82	CPL	41.02± 1.42	–0.36± 0.05	529.6± 21.9	...	606.85	585	40.32± 1.20
091003191	23.552	18.05	19.07	CPL	74.52± 2.32	–0.80± 0.03	492.0± 21.6	...	334.67	355	59.10± 1.50
091005679	16.384	1.02	2.05	CPL	11.72± 4.06	–0.53± 0.27	203.5± 44.0	...	733.32	596	2.65± 0.39
091010113	9.216	1.92	2.94	CPL	302.70± 14.10	–0.58± 0.03	146.1± 3.05	...	342.57	357	43.94± 0.63
091012783	0.832	0.00	0.06	CPL	55.57± 5.40	–0.25± 0.15	994.9± 154.0	...	304.50	353	171.08± 21.51
091019750	0.32	–0.06	0.00	CPL	51.58± 14.00	–0.32± 0.23	269.5± 53.4	...	523.10	590	16.48± 2.60
091020900	28.672	2.56	3.58	CPL	17.18± 1.27	–1.17± 0.07	743.3± 196.0	...	389.24	357	18.83± 2.65
091020977	49.153	0.80	1.82	CPL	20.45± 0.86	–0.52± 0.06	771.0± 68.5	...	794.17	713	33.37± 2.20
091030613	34.816	13.82	14.85	CPL	46.69± 14.20	–0.26± 0.21	121.8± 9.89	...	587.18	595	3.64± 0.25
091030828	41.086	17.54	18.56	Band	29.53± 1.32	–0.58± 0.06	698.3± 64.1	–2.39± 0.18	476.03	469	62.51± 7.00
091031500	43.009	6.91	7.94	CPL	19.92± 1.17	–0.94± 0.06	585.6± 77.9	...	973.13	830	18.73± 1.50
091101143	16.384	3.84	4.86	CPL	119.40± 12.00	–0.28± 0.07	156.9± 5.88	...	377.67	355	14.73± 0.44
091103912	25.6	0.00	1.79	CPL	33.45± 2.67	–0.47± 0.07	272.0± 16.7	...	490.00	476	11.42± 0.50
091107635	11.264	0.00	2.05	CPL	16.48± 4.77	–0.65± 0.19	133.1± 16.9	...	668.17	596	2.24± 0.19
091109895	24.5765	0.51	1.54	CPL	41.47± 7.57	–0.72± 0.11	128.2± 10.6	...	525.39	476	5.80± 0.31
091120191	59.393	26.62	27.65	CPL	96.34± 7.23	–0.90± 0.05	122.2± 4.53	...	633.30	596	15.70± 0.35
091123298	367.175	11.26	12.29	CPL	16.07± 2.10	–1.19± 0.09	329.0± 82.2	...	396.50	352	8.83± 2.18
091126333	0.384	–0.06	0.00	CPL	63.01± 15.30	–0.31± 0.24	303.8± 55.2	...	419.27	480	24.60± 3.21
091126389	0.032	–0.02	0.02	CPL	61.79± 9.66	–0.20± 0.17	616.4± 97.40	...	616.74	715	84.63± 11.00
091127976	13.054	0.00	1.79	Band	754.50± 80.80	–0.68± 0.05	59.67± 1.81	–2.12± 0.01	555.62	469	93.79± 2.30
091128285	138.243	6.91	7.94	CPL	48.14± 3.99	–0.48± 0.07	311.5± 23.1	...	427.53	354	20.27± 1.10
091207333	27.648	6.14	7.17	CPL	18.42± 5.68	–0.59± 0.21	145.7± 20.8	...	833.72	721	2.68± 0.26
091208410	13.312	7.81	8.83	CPL	68.01± 4.13	–1.10± 0.04	227.4± 16.2	...	387.41	350	25.62± 0.97

Table 4. continued.

GRB	Δt s	t_1 s	t_2 s	Model	[a] A/10^{-3} ph/cm^2/s	α	$E_{\rm peak}$ keV	β	C–stat	d.o.f.	Flux/10^{-7} erg/cm^2/s
091209001	52.225	12.29	13.31	CPL	151.10± 95.40	–0.33± 0.31	54.08± 4.61	...	244.66	237	3.17± 0.23
091220442	25.6	2.82	3.84	CPL	22.68± 2.62	–1.24± 0.07	143.40± 13.70	...	655.82	598	6.43± 0.30
091221870	39.937	14.34	15.36	CPL	14.59± 1.14	–1.00± 0.07	662.3± 138.0	...	488.99	470	15.29± 1.90
091223511	65.537	5.12	6.14	CPL	9.67± 2.29	–0.12± 0.31	335.2± 58.5	...	757.92	715	4.38± 0.59
091227294	35.84	2.82	3.84	CPL	15.84± 2.10	–0.81± 0.11	349.7± 63.0	...	487.51	475	8.32± 0.95
091231206	60.417	5.63	6.66	CPL	44.93± 9.80	–0.25± 0.16	158.5± 13.4	...	608.25	595	5.50± 0.37
100116897	47.1047	93.19	94.21	CPL	40.16± 0.71	–1.02± 0.02	1645.0± 130.0	...	505.07	473	102.75± 5.50
100117879	0.256	0.00	0.06	CPL	51.66± 14.10	0.35± 0.40	333.5± 50.3	...	467.21	479	22.66± 3.10
100118100	7.168	1.02	2.05	CPL	8.35± 0.76	–0.64± 0.13	1144.0± 292.0	...	494.82	474	21.56± 4.10
100122616	30.7206	20.48	21.50	Band	249.20± 34.90	–1.13± 0.06	56.88± 2.68	–2.41± 0.05	581.98	468	39.57± 1.60
100130729	74.7536	72.71	73.73	CPL	22.41± 2.84	–0.99± 0.08	232.7± 31.7	...	616.42	590	8.02± 0.59
100131730	11.645	0.00	1.41	Band	171.60± 10.80	–0.38± 0.04	172.4± 5.82	–2.76± 0.11	426.64	466	35.69± 1.50
100204024	83.97	5.12	6.14	CPL	16.96± 2.33	–1.02± 0.09	226.2± 33.6	...	815.31	703	6.02± 0.49
100205490	17.408	0.00	0.51	CPL	23.92± 9.19	–0.44± 0.28	178.1± 35.3	...	385.32	354	4.13± 0.60
100206563	0.256	0.00	0.06	CPL	88.74± 6.80	–0.28± 0.10	621.9± 65.5	...	531.77	479	118.10± 9.67
100208386	0.32	–0.06	0.00	CPL	8.94± 2.21	–0.26± 0.29	1843.0± 620.0	...	420.14	473	80.24± 24.01
100211440	33.792	10.24	11.26	CPL	44.06± 5.69	–1.08± 0.09	151.1± 12.1	...	403.50	352	10.94± 0.49
100212550	8.192	0.00	1.09	CPL	24.32± 3.70	0.46± 0.22	303.1± 23.2	...	475.96	474	8.42± 0.58
100218194	40.961	4.10	5.12	CPL	9.58± 4.71	–0.30± 0.42	147.6± 22.5	...	680.65	594	1.08± 0.14
100223110	0.384	0.13	0.19	CPL	33.66± 3.46	0.22± 0.14	1279.0± 114.0	...	453.62	477	292.85± 24.75
100224112	53.2489	16.38	17.41	CPL	74.03± 8.79	–0.56± 0.08	176.5± 11.4	...	414.48	357	13.89± 0.58
100225115	27.648	6.40	7.42	CPL	15.41± 1.16	–0.51± 0.09	539.7± 63.9	...	737.36	720	14.87± 1.21
100225580	13.312	2.56	3.58	CPL	49.48± 3.14	–0.79± 0.05	265.6± 17.3	...	645.39	602	18.46± 0.75
100225703	16.384	0.00	1.54	CPL	12.10± 1.65	–0.11± 0.17	365.5± 42.6	...	811.51	709	6.45± 0.60
100301068	0.192	–0.06	0.00	CPL	45.49± 10.60	–0.41± 0.22	358.7± 71.2	...	315.52	354	23.63± 3.70
100301223	36.865	7.17	8.19	CPL	29.90± 13.80	–0.65± 0.26	89.96± 11.7	...	329.89	350	2.35± 0.21
100304534	21.504	3.07	4.10	CPL	33.46± 9.23	–0.72± 0.17	124.2± 15.0	...	400.68	357	4.50± 0.36
100311518	13.312	2.56	3.58	CPL	9.52± 2.16	–0.45± 0.24	378.1± 93.7	...	462.73	472	5.38± 1.04
100313288	19.456	1.54	2.56	CPL	41.77± 6.13	–0.34± 0.12	202.7± 16.0	...	457.45	480	8.32± 0.51
100318611	21.504	3.58	4.61	CPL	317.50±423.00	0.21± 0.64	41.66± 3.7	...	485.00	475	1.35± 0.13
100322045	41.985	31.75	32.77	CPL	48.61± 1.32	–0.67± 0.03	675.9± 34.4	...	488.27	479	60.23± 2.10
100323542	38.9126	52.22	53.25	CPL	15.78± 2.85	–0.52± 0.17	293.8± 43.5	...	391.23	358	6.13± 0.64
100324172	21.118	4.74	5.76	CPL	151.00± 4.33	–0.39± 0.03	332.2± 8.24	...	529.59	477	69.21± 1.30
100325246	19.456	0.00	1.79	CPL	20.66± 10.10	–1.12± 0.24	50.64± 5.46	...	317.98	358	1.81± 0.13
100325275	9.216	0.00	1.41	CPL	41.58± 6.27	–0.01± 0.14	233.2± 18.3	...	495.98	477	9.06± 0.59
100326402	125.954	13.31	14.34	CPL	10.47± 1.76	–0.93± 0.14	335.6± 78.9	...	534.37	476	5.40± 0.75
100328141	0.768	–0.06	0.00	CPL	30.35± 2.86	–0.42± 0.13	1203.0± 275.0	...	589.26	597	107.06± 21.01
100330309	22.528	1.54	2.56	CPL	41.63± 5.77	–0.68± 0.09	160.5± 11.7	...	636.75	587	7.57± 0.34

Notes. [(a)] For all models the pivot energy for the amplitude is 100 keV. The flux is computed in the 8 keV–35 MeV energy range.

Table 5. Spectral parameters of the *Fermi*/GBM GRBs collected from the GCN Circular Archive.

GRB	z	Δt s	E_{peak} keV	α	β	Fluence erg/cm^2	Range keV	GCN* number
080810549	3.35	50	313.5 ±73.6	-0.91 ± 0.12	...	6.9e-6 ± 0.5e-6	50-300	(8083)8100
080816503	...	70	146.7 ±14.5	-0.57 ± 0.14	...	1.86e-5 ± 0.20e-5	50-300	8107
080816989	...	5	1230 ±230	-0.37 ± 0.17	...	7.23e-7 ± 4.2e-8	25-1000	8111
080817720	...	6	...	-1.07 ± 0.04	...	2.6e-6 ± 0	25-1000	8109
080818579	...	50	...	-1.57 ± 0.05	...	2.26e-6 ± 0	50-300	8110
080818945	...	10	80 ±11	-1.3 ± 0.1	...	1.e-6 ± 0	50-300	8116
080823363	...	46	164.7 ±34.2	-1.2 ± 0.2	...	4.1e-6 ± 0	50-300	8145
080824909	...	28	100 ±16	-0.4 ± 0.2	-2.1 ± 0.2	2.3e-6 ± 0	50-300	8144
080825593	...	22	155 ±5	-0.39 ± 0.04	-2.34± 0.09	2.4e-5 ± 0	50-300	8141
080830368	...	45	280 ±63	-0.88 ± 0.12	...	4.6e-6 ± 0	50-300	8167
080904886	...	22	35 ±1	0.0 ± 0.17	-2.7 ± 0.08	2.25e-6 ± 0.49e-6	50-300	8206
080905499	...	1	...	-0.96 ± 0.05	...	2.8e-7 ± 0.2e-7	50-300	8204
080905570	...	28	78.8 ±5.9	-0.90 ± 0.17	...	4.6e-6 ± 0.3e-6	25-1000	8213
080905705	2.374	159	...	-1.75 ± 0.12	...	4.1e-8 ± 0.3e-8	20-1000	(8191) 8205
080906212	...	5	125.3 ±6.6	-0.07 ± 0.09	-2.10± 0.07	10.9e-6 ± 0.1e-6	25-1000	8214
080912360	...	17	...	-1.74 ± 0.07	...	3.3e-6 ± 0.1e-6	25-1000	8235
080913735	...	140	114 ±14	-0.69 ± 0.16	...	2.2e-6 ± 0.5-6	50-300	8280
080916009	4.35	66	424 ±24	-0.91 ± 0.02	-2.08± 0.06	1.9e-4 ± 0	8-30000	(a) 8278
080916406	0.689	60	109 ±9	-0.9 ± 0.1	...	1.5e-5 ± 0.5e-5	25-1000	(8254) 8263
080920268	...	85	162 ±35	-0.63 ± 0.25	...	2.4e-6 ± 0.5e-6	25-1000	8290
080925775	...	29	120 ±5	-0.53 ± 0.05	-2.26± 0.08	9.7e-6 ± 0	50-300	8291
080927480	...	25	...	-1.5 ± 0.1	...	5.7e-6 ± 0.2e-6	25-1000	8302
080928628	1.692	87	...	-1.80 ± 0.08	...	1.5e-6 ± 0.1e-6	50-300	(8301) 8316
081003644	...	67	...	-1.41 ± 0.06	...	5.4e-6 ± 0	50-300	8329
081006604	...	7	1135 ±826	-0.77 ± 0.24	-1.80± 0.22	7.1e-7 ± 0	50-300	8341
081006872	...	9	...	-1.30 ± 0.09	...	7.3e-7 ± 0	50-300	8341
081007224	0.5295	12	...	-2.1 ± 0.1	-10 ± -10	1.2e-6 ± 0.1e-6	25-900	(8335) 8369
081009140	...	22	35 ±1	0.15 ± 0.1	-3.5 ± 0.1	4.33e-5 ± 0.15e-5	8-1000	8374
081012549	...	30	360 ±70	-0.31 ± 0.23	...	3.8e-6 ± 0.4e-6	25-900	8370
081021398	...	25	117 ±11	0.11 ± 0.25	-2.8 ± 0.4	5.3e-6 ± 0.6e-6	10-1000	8432
081024851	...	65	65 ±7	-0.6 ± 0.2	-2.5 ± 0.2	4.0e-6 ± 0.9e-6	50-300	8498
081024891	...	0.8	1583 ±520	-0.70 ± 0.13	...	3.4e-7 ± 0.1e-7	50-300	8408
081025349	...	45	251 ±25	-0.35 ± 0.13	...	7.1e-6 ± 0.5e-6	8-1000	8483
081028538	...	20	70 ±4	-0.55 ± 0.16	...	2.0e-6 ± 0.3e-6	10-1000	8433
081101532	...	8	550 ±30	-0.62 ± 0.05	...	1.60e-5 ± 0.03e-5	8-1000	8486
081102365	...	2.2	...	-1.07 ± 0.06	...	1.12e-6 ± 0.04e-6	8-1000	8496
081102739	...	88	88.7 ±8.3	0.0 ± 0.3	...	2.1e-6 ± 0.05e-6	50-300	8476
081105614	...	0.18	...	-1.17 ± 0.05	...	2.28e-7 ± 0.11e-7	8-1000	8495
081107321	...	2.2	65 ±3	0.25 ± 0.17	-2.80± 0.15	1.64e-6 ± 0.28e-6	8-1000	8494
081109293	...	45	240 ±60	-1.28 ± 0.09	...	6.53e-6 ± 0.43e-6	8-1000	8505
081113230	...	0.5	...	-1.28 ± 0.05	...	1.07e-6 ± 0.03e-6	8-1000	8521
081118876	...	20	41.2 ±3.9	0.8 ± 0.5	-2.14± 0.08	1.12e-7 ± 0.61e-7	8-1000	8550
081119184	...	0.8	...	-1.3 ± 0.1	...	4.1e-7 ± 0.2e-7	8-1000	8533
081120618	...	12	44 ±5	0.4 ± 0.5	-2.18± 0.10	2.7e-6 ± 0.9e-6	8-1000	8551
081122520	...	26	200.7 ±15.7	-0.77 ± 0.07	...	9.6e-6 ± 1.1e-6	8-1000	8549
081122614	...	0.3	...	-1.5 ± 0.1	...	7.9e-8 ± 0.1e-8	50-300	8579
081124060	...	35	21.0 ±6.0	-1.5 ± 0.2	...	1.13e-5 ± 0.2e-5	8-1000	8552
081126899	...	56	176 ±84	-0.3 ± 0.5	-1.7 ± 0.1	1.5e-7 ± 0.6e-7	8-1000	8589
081129161	...	59	150 ±30	-0.5 ± 0.2	-1.84± 0.08	2.0e-5 ± 0.3e-5	8-1000	8586
081130629	...	12	152 ±17	-0.77 ± 0.12	...	1.3e-6 ± 0.1e-6	50-300	8593
081204004	...	4.7	...	-1.4 ± 0	...	1.48e-6 ± 0.3e-6	8-1000	8710
081204517	...	0.32	...	-1.18 ± 0.05	...	4.88e-7 ± 0.13e-7	8-1000	8622
081206275	...	24	180 ±23	-0.11 ± 0.24	...	4.0e-6 ± 0.6e-6	8-1000	8640
081206987	...	20	...	-1.35 ± 0.04	...	1.19e-6 ± 0.04e-6	50-300	8644
081207680	...	153	639 ±42	-0.65 ± 0.03	-2.41± 0.17	1.06e-4 ± 0.2e-4	10-1000	8665
081209981	...	0.4	808 ±163	-0.5 ± 0.1	-2.0 ± 0.1	5.9e-7 ± 0.3e-7	8-1000	8664
081215784	...	7.7	304 ±11	-0.585 ± 0.022	-2.06± 0.038	5.44e-5 ± 0.07e-5	8-1000	8678
081215880	...	20	139 ±14	-0.14 ± 0.26	...	2.8e-6 ± 0.5e-6	8-1000	8682
081216531	...	0.96	1235 ±264	-0.70 ± 0.09	-2.17± 0.21	3.6e-6 ± 0.1e-6	10-1000	8680
081217983	...	39	167 ±11	-0.61 ± 0.09	-2.7 ± 0.6	1.0e-5 ± 0.07e-5	8-1000	8686
081221681	...	40	77 ±1	-0.42 ± 0.03	-2.91± 0.08	3.7e-5 ± 0.1e-5	8-1000	8704
081222204	2.77	30	134 ±9	-0.55 ± 0.07	-2.10± 0.06	1.35e-5 ± 0.08e-5	8-1000	(8713) 8715
081223419	...	0.89	280 ±30	-0.63 ± 0.10	...	1.20e-6 ± 0.10e-6	8-1000	8720
081225256	...	42	...	-1.51 ± 0.04	...	2.45e-6 ± 0.06e-6	50-300	8784
081226044	...	1.7	...	-1.17 ± 0.08	...	2.1e-7 ± 0.1e-7	50-300	8785

Table 5. continued.

GRB	z	Δt s	E_{peak} keV	α	β	Fluence erg/cm^2	Range keV	GCN* number
081226156	...	60	82 ±7	-1.04 ± 0.11	...	2.32e-6 ± 0.24e-6	8-1000	8750
081226509	...	0.35	530 ±110	-0.51 ± 0.17	...	6.1e-7 ± 0.5e-7	8-1000	8751
081229187	...	0.5	807 ±186	-0.42 ± 0.18	...	8.7e-7 ± 0.8e-7	8-1000	8775
081231140	...	29	152.3 ±11.9	-0.80 ± 0.06	-2.03± 0.07	1.2e-5 ± 5.9e-7	8-1000	8781
090107681	...	24.1	106.1 ±14.8	-0.68 ± 0.26	...	1.75e-6 ± 0.37e-6	8-1000	8793
090108020	...	0.90	104.8 ±16.4	-0.47 ± 0.20	-1.97± 0.09	1.28e-6 ± 0.24e-6	8-1000	8798
090108322	...	0.8	...	-0.99 ± 0.06	...	7.9e-7 ± 0.4e-7	8-1000	8801
090109332	...	5	...	-1.50 ± 0.08	...	1.21e-6 ± 0.05e-6	8-1000	8802
090112332	...	65	150 ±40	-0.94 ± 0.20	-2.01± 0.19	5.2e-6 ± 1.0e-6	8-1000	8803
090112729	...	12	139 ±9	-0.75 ± 0.06	-2.43± 0.14	5.4e-6 ± 0.3e-6	8-1000	8805
090117335	...	27	...	-1.55 ± 0.08	...	2.1e-6 ± 0.1e-6	8-1000	8824
090117632	...	86	247 ±41	-1.0 ± 0.1	-2.1 ± 0.2	1.1e-5 ± 0.1e-5	8-1000	8822
090117640	...	21	25 ±2	-0.4 ± 0.5	-2.5 ± 0.1	1.8e-6 ± 1.3e-6	8-1000	8821
090126227	...	10.8	47.5 ±3.4	-0.99 ± 0.18	...	1.25e-6 ± 0.24e-6	8-1000	8853
090129880	...	17.2	123.2 ±44.8	-1.39 ± 0.13	-1.98± 0.14	5.6e-6 ± 0.7e-6	8-1000	8897
090131090	...	36.4	58.4 ±3.9	-1.27 ± 0.07	-2.26± 0.05	2.23e-5 ± 0.17e-5	8-1000	8876
090202347	...	66	570 ±170	-1.31 ± 0.06	...	8.65e-6 ± 0.31e-6	8-1000	8877
090206620	...	0.8	710 ±170	-0.65 ± 0.14	...	1.04e-6 ± 0.06e-6	8-1000	8916
090207777	...	10	...	-1.59 ± 0.04	...	4.01e-6 ± 0.09e-6	8-1000	8899
090217206	...	32.8	626 ±29	-0.85 ± 0.02	...	3.08e-5 ± 0.03e-5	8-1000	8902
090219074	...	0.5	0.....0	-1.43 ± 0.05	...	8.0e-7 ± 0.4e-7	8-1000	8911
090222179	...	18	157.7 ±19.8	-1.00 ± 0.11	...	2.19e-6 ± 0.19e-6	8-1000	8912
090227310	...	50	1355 ±259	-0.91 ± 0.06	...	9.0e-6 ± 0.2e-6	8-1000	8917
090227772	...	0.9	2255 ±116	-0.53 ± 0.02	-3.04± 0.23	0.87e-5 ± 0.01e-5	10-1000	8921
090228204	...	0.8	849 ±44	-0.35 ± 0.04	-2.98± 0.25	6.1e-6 ± 0.09e-6	8-1000	8918
090228976	...	7.232	147.8 ±34.1	-0.6963± 0.293	...	9.96e-7 ± 0.22e-7	8-1000	8927
090301315	...	28	546 ±133	-1.03 ± 0.09	...	2.69e-6 ± 0.13e-6	8-1000	8922
090305052	...	2.	770 ±230	-0.5 ± 0.17	-1.9 ± 0.2	2.7e-6 ± 0.2e-6	8-1000	8972
090306245	...	38.8	107 ±16	-0.58 ± 0.29	...	9.0e-7 ± 2.2e-7	8-1000	8960
090307167	...	30	212 ±80	-0.7 ± 0.3	...	1.7e-6 ± 0.4e-6	8-1000	8961
090308734	...	2.11	710.3 ±100.0	-0.54 ± 0.11	...	3.46e-6 ± 0.13e-6	8-1000	8963
090309767	...	35.	197 ±65	-1.52 ± 0.1	...	4.7e-6 ± 0.4e-6	8-1000	8971
090310189	...	125.2	279 ±43	-0.65 ± 0.13	...	2.15e-6 ± 0.17e-6	8-1000	8977
090319622	...	67.7	187.3 ±20.4	-0.9 ± 0.1	...	7.47e-6 ± 0.53e-6	8-1000	9019
090320801	...	52	72 ±14	-1.1 ± 0.3	...	1.1e-6 ± 0.3e-6	8-1000	9020
090323002	3.57	70	697 ±51	-0.89 ± 0.03	...	1.e-4 ± 0.01e-4	8-1000	(9028) 9035
090326633	...	11.2	75 ±8	-0.86 ± 0.22	...	8.6e-7 ± 1.8e-7	8-1000	9059
090327404	...	24	96.4 ±5.1	-0.5 ± 0.12	...	3.0e-6 ± 0.4e-6	8-1000	9040
090328401	0.736	50	653 ±45	-0.93 ± 0.02	-2.2 ± 0.1	8.09e-5 ± 0.1e-5	8-1000	(9053) 9057
090328713	...	0.32	1967 ±701	-0.92 ± 0.06	-2.48± 0.66	9.61e-7 ± 0.31e-7	8-1000	9056
090330279	...	80	261 ±18	-1.01 ± 0.04	...	1.14e-5 ± 0.03e-5	8-1000	9055
090409288	...	20	137 ±17	1.2 ± 0.7	...	6.14e-7 ± 0.26e-7	8-1000	9119
090411838	...	24.6	141 ±35	-0.88 ± 0.15	-1.82± 0.08	8.6e-6 ± 1.2e-6	8-1000	9130
090411991	...	18.7	189 ±37	-0.8 ± 0.1	-2.0 ± 0.2	8.e-6 ± 0.8e-6	8-1000	9131
090418816	...	0.6	...	-1.27 ± 0.04	...	6.0e-7 ± 0.3e-7	8-1000	9184
090422150	...	10	...	-1.81 ± 0.15	...	1e-6 ± 0.1e-6	8-1000	9228
090423330	8.1	12	82 ±15	-0.77 ± 0.35	...	1.1e-6 ± 0.3e-6	8-1000	(b) 9229
090424592	0.544	52	177 ±3	-0.9 ± 0.02	-2.9 ± 0.1	5.2e-5 ± 0.1e-5	8-1000	(9243) 9230
090425377	...	72	142 ±13	-1.56 ± 0.04	...	1.3e-5 ± 0.2e-5	8-1000	9271
090426066	...	3.8	...	-1.6 ± 0.08	...	5.2e-7 ± 1.2e-7	8-1000	9299
090426690	...	12	351 ±110	-1.31 ± 0.09	...	3.1e-6 ± 0.2e-6	8-1000	9300
090427644	...	7	...	-1.1 ± 0.1	...	8e-7 ± 0.5e-7	8-1000	9301
090427688	...	12.5	75 ±3	0.35 ± 0.16	...	1.6e-6 ± 0.2e-6	8-1000	9302
090428441	...	8	97 ±7	-0.59 ± 0.16	...	9.9e-7 ± 1.4e-7	8-1000	9294
090428552	...	30	65 ±16	-1.86 ± 0.07	...	5.2e-6 ± 0.3e-6	8-1000	9295
090429530	...	13	...	-1.43 ± 0.04	...	3.7e-6 ± 0.1e-6	8-1000	9310
090429753	...	11	223 ±72.5	-0.87 ± 0.27	...	1.6e-6 ± 0.3e-6	8-1000	9311
090502777	...	66.2	63.2 ±8.7	-1.1 ± 0.3	...	3.5e-8 ± 0.9e-8	8-1000	9346
090510016	0.903	1	4400 ±400	-0.80 ± 0.03	-2.6 ± 0.3	3.0e-5 ± 0.2e-5	8-40000	(9353) 9336
090511684	...	14	391 ±157	-0.95 ± 0.18	...	1.8e-6 ± 0.2e-6	8-1000	9399
090513916	...	23	850 ±390	-0.9 ± 0.1	...	6.8e-6 ± 0.4e-6	8-1000	9390
090514006	...	49	...	-1.92 ± 0.04	...	8.1e-6 ± 0.2e-6	8-1000	9398
090516137	...	140	327 ±58.7	-1.01 ± 0.06	...	3.0e-5 ± 0.1e-5	8-1000	9413
090518080	...	9	...	-1.59 ± 0.06	...	1.6e-6 ± 0.05e-6	8-1000	9419
090518244	...	12	127 ±12	-0.74 ± 0.13	...	2.2e-6 ± 0.2e-6	8-1000	9392
090519462	...	87	...	-1.63 ± 0.05	...	1.4e-6 ± 0.01e-6	8-1000	9412

Table 5. continued.

GRB	z	Δt s	E_{peak} keV	α	β	Fluence erg/cm^2	Range keV	GCN* number
090520832	...	1.5	...	-1.4 ± 0.1	...	4.5e-7 ± 0.2e-7	8-1000	9427
090520850	...	4.9	204.2 ±27.9	-0.73 ± 0.09	-1.96± 0.1	3.54e-6 ± 0.25e-6	8-1000	9428
090520876	...	12	47.4 ±4.1	-1.03 ± 0.22	...	4.e-6 ± 0.9e-6	8-1000	9429
090522344	...	22	75.8 ±24.2	-1.03 ± 0.46	...	1.2e-6 ± 0.3e-6	8-1000	9425
090524346	...	72	82.6 ±6.3	-1.00 ± 0.08	-2.3 ± 0.09	1.85e-5 ± 0.15e-5	8-1000	9424
090528516	...	102	172 ±12	-1.1 ± 0.04	-2.3 ± 0.1	4.65e-5 ± 0.15e-5	8-1000	9447
090529564	...	10.4	188 ±15	-0.84 ± 0.05	-2.1 ± 0.1	3.1e-6 ± 0.1e-6	8-1000	9474
090530760	...	194	67 ±3	-0.71 ± 0.06	-2.42± 0.05	5.9e-5 ± 0.4e-5	8-1000	9472
090531775	...	2	2166 ±525	-0.71 ± 0.10	-2.47± 0.35	6.20e-7 ± 0.18e-7	8-1000	9501
090602564	...	16	503 ±91	-0.56 ± 0.14	...	5.7e-6 ± 0.3e-6	8-1000	9486
090606471	...	60	...	-1.63 ± 0.09	...	3.19e-6 ± 0.16e-6	8-1000	9497
090608052	...	61	...	-1.83 ± 0.07	...	3.2e-6 ± 0.1e-6	8-1000	9498
090610648	...	6.5	...	-1.3 ± 0.03	...	7.32e-7 ± 0.24e-7	8-1000	9507
090610883	...	18.1	...	-1.62 ± 0.08	...	8.54e-7 ± 0.38e-7	8-1000	9508
090612619	...	58	357 ±59	-0.6 ± 0.1	-1.9 ± 0.1	2.37e-6 ± 0.14e-6	8-1000	9510
090616157	...	2.7	...	-1.27 ± 0.07	...	2.23e-7 ± 0.09e-7	8-1000	9511
090617208	...	0.45	684 ±225	-0.45 ± 0.2	-2.0 ± 0.22	4.68e-7 ± 0.2e-7	8-1000	9523
090618353	0.54	155.	155.5 ±11.	-1.26 ± 0.04	-2.5 ± 0.25	2.7e-4 ± 0.06e-4	8-1000	(9518) 9535
090620400	...	16.5	156 ±6	-0.4 ± 0.04	-2.44± 0.1	6.6e-6 ± 0.2e-6	8-1000	9554
090621185	...	294	56.0 ±10.7	-1.1 ± 0.2	-2.12± 0.09	4.4e-6 ± 1.0e-6	8-1000	9556
090621417	...	59.9	148 ±34	-1.4 ± 0.1	...	1.8e-6 ± 0.2e-6	8-1000	9558
090621447	...	39.9	...	-1.66 ± 0.05	...	1.34e-6 ± 0.03e-6	8-1000	9560
090621922	...	0.128	321.6 ±129	-0.13 ± 0.38	-1.57± 0.08	3.71e-7 ± 0.58e-7	8-1000	9562
090623107	...	72.2	476 ±39	-0.73 ± 0.04	...	9.6e-6 ± 0.02e-6	8-1000	9566
090625234	...	51	198 ±36	-0.6 ± 0.2	...	8.8e-7 ± 1.2e-7	8-1000	9571
090625560	...	13.6	165 ±28	-0.9 ± 0.2	...	1.04e-6 ± 0.13e-6	8-1000	9583
090626189	...	70	175 ±12	-1.29 ± 0.02	-1.98± 0.02	3.5e-5 ± 0.1e-5	8-1000	9579
090630311	...	5.1	79 ±13	-1.5 ± 0.1	...	5.1e-7 ± 0.7e-7	8-1000	9598
090701225	...	12	...	-1.84 ± 0.09	...	4.5e-7 ± 0.0	8-1000	9600
090703329	...	9	...	-1.72 ± 0.06	...	6.8e-7 ± 0.2e-7	8-1000	9608
090704242	...	70	233.7 ±32	-1.13 ± 0.07	...	5.8e-6 ± 0.3e-6	8-1000	9627
090706283	...	100	...	-2.16 ± 0.09	...	1.5e-6 ± 0.1e-6	8-1000	9619
090708152	...	18	47.5 ±11	-1.29 ± 0.36	...	4.e-7 ± 0	8-1000	9631
090709630	...	32	130 ±24	-1.01 ± 0.16	...	1.3e-6 ± 0.2e-6	8-1000	9650
090711850	...	100	210 ±70	-1.3 ± 0.1	...	1.17e-5 ± 0.16e-5	8-1000	9713
090712160	...	72	505 ±101	-0.68 ± 0.13	...	4.2e-6 ± 0.3e-6	8-1000	9662
090713020	...	113	99 ±5	-0.34 ± 0.12	...	3.7e-6 ± 0.4e-6	8-1000	9661
090717034	...	70	120 ±5	-0.88 ± 0.04	-2.33± 0.06	4.5e-7 ± 0.2e-7	8-1000	9692
090717111	...	0.9	...	-1.02 ± 0.04	...	4.83e-7 ± 0.03e-7	8-1000	9693
090718762	...	28	198 ±9	-1.21 ± 0.02	...	2.52e-5 ± 0.05e-5	8-1000	9690
090719063	...	16	254 ±6	-0.68 ± 0.02	-2.92± 0.16	4.83e-5 ± 0.04e-5	8-1000	9691
090720276	...	7	117.5 ±7.12	-0.75 ± 0.1	...	2.9e-6 ± 0.1e-6	8-1000	9688
090720710	...	20	982 ±186	-1.01 ± 0.05	...	1.06e-5 ± 0.03e-5	8-1000	9698
090802235	...	0.128	283 ±55	-0.42 ± 0.19	-2.4 ± 0.5	6.5e-7 ± 0.3e-7	8-1000	9742
090807832	...	3	37 ±5	-0.6 ± 0.4	-2.4 ± 0.1	1.02e-6 ± 0.07e-6	8-1000	9767
090809978	...	15	198 ±13	-0.85 ± 0.04	-2.02± 0.06	2.26e-5 ± 0.03e-5	8-1000	9760
090813174	...	9	161 ±26	-1.43 ± 0.08	...	3.5e-6 ± 0.2e-6	8-1000	9792
090814368	...	0.25	790 ±120	-0.39 ± 0.11	...	6.6e-7 ± 0.4e-7	8-1000	9804
090815300	...	200	...	-1.5 ± 0.1	...	3.4e-6 ± 0.3e-6	8-1000	9812
090815438	...	30	15.1 ±10.8	-1.89 ± 0.12	...	5.05e-6 ± 0.25e-6	8-1000	9813
090817036	...	220	115 ±50	-1.1 ± 0.3	-2.2 ± 0.6	7.3e-6 ± 0.1e-6	8-1000	9823
090820027	...	30	215 ±3	-0.69 ± 0.01	-2.61± 0.05	6.6e-5 ± 0.1e-5	8-1000	9829
090820509	...	11.2	38.8 ±4.4	-1.44 ± 0.18	...	1.16e-6 ± 0.07e-6	8-1000	9832
090826068	...	8.5	172 ±100	-0.96 ± 0.3	...	1.26e-6 ± 0.27e-6	8-1000	9845
090828099	...	100	136.5 ±15	-1.23 ± 0.05	-2.12± 0.1	2.52e-5 ± 0.08e-5	8-1000	9844
090829672	...	85	183 ±31	-1.44 ± 0.04	-2.1 ± 0.1	1.02e-4 ± 0.02e-4	8-1000	9849
090829702	...	100	143 ±30	-0.7 ± 0.2	-2.4 ± 0.5	6.4e-6 ± 0.7e-6	8-1000	9856
090831317	...	69.1	399.6 ±86.2	-1.57 ± 0.03	...	1.66e-5 ± 0.05e-5	8-1000	9850
090902401	...	1.2	388 ±90	0.3 ± 0.35	-2.05± 0.26	2.11e-6 ± 0.14e-6	8-1000	9865
090902462	1.822	21	798 ±7	-0.61 ± 0.01	-3.87± 0.16	3.74e-4 ± 0.03e-4	8-1000	(9873) 9866
090904058	...	71	106.3 ±24.6	-1.26 ± 0.15	-2.18± 0.18	2.44e-5 ± 0.15e-5	8-1000	9895
090910812	...	62	274.8 ±56.1	-0.9 ± 0.1	-2.0 ± 0.2	9.2e-6 ± 0.7e-6	8-1000	9904
090922539	...	92	139.3 ±6.6	-0.77 ± 0.05	-2.28± 0.07	1.14e-5 ± 0.02e-5	8-1000	9929
090925389	...	50	156 ±22	-0.6 ± 0.14	-1.9 ± 0.08	9.46e-6 ± 0.26e-6	8-1000	9932
090926181	2.1062	20	268 ±4	-0.693 ± 0.01	-2.34± 0.011	1.45e-4 ± 0.04e-4	8-1000	(9942) 9972
090926914	1.24	81	91 ±2	-0.13 ± 0.06	...	8.7e-6 ± 0.3e-6	8-1000	9957

Table 5. continued.

GRB	z	Δt s	E_{peak} keV	α	β	Fluence erg/cm^2	Range keV	GCN* number
090927422	1.37	2	...	-1.47 ± 0.06	...	6.1e-7 ± 0.5e-7	8-1000	9974
090929190	...	8.5	610.9 ±44.5	-0.52 ± 0.06	...	1.06e-5 ± 0.03e-5	8-1000	9962
091003191	...	21.1	486.2 ±23.6	-1.13 ± 0.01	-2.64± 0.24	3.76e-5 ± 0.04e-5	8-1000	9983
091010113	...	8.1	150 ±6	-1.11 ± 0.03	...	1.09e-5 ± 0.02e-5	8-1000	10018
091020900	1.71	37	47.9 ±7.1	0.2 ± 0.4	-1.7 ± 0.2	1e-5 ± 0.2e-5	8-1000	(10053) 10095
091030828	...	160	507 ±30	-0.88 ± 0.02	-2.2 ± 0.1	3.03e-5 ± 4.3e-7	8-1000	10146
091031500	...	35	503.1 ±47	-0.91 ± 0.04	-2.34± 0.25	2.05e-5 ± 0.04e-5	8-1000	10115
091102607	...	7.3	...	-1.24 ± 0.03	...	2.1e-6 ± 0.1e-6	8-1000	10126
091112737	...	40	750 ±120	-1.13 ± 0.04	...	9.7e-6 ± 0.3e-6	10-1000	10164
091120191	...	52	129 ±3	-1.17 ± 0.02	...	3.02e-5 ± 0.04e-5	8-1000	10187
091123298	...	650	101.3 ±5	-1.08 ± 0.05	...	4.07e-5 ± 0.09e-5	8-1000	10226
091126333	...	0.3	458 ±160	-0.6 ± 0.23	...	5.9e-7 ± 0.5e-7	8-1000	10223
091126389	...	0.03	731 ±200	-0.23 ± 0.28	...	2.2e-7 ± 0.02e-7	8-1000	10225
091127976	0.49	9	36 ±2	-1.27 ± 0.06	-2.2 ± 0.02	1.87e-5 ± 0.02e-5	8-1000	(10202) 10204
091128285	...	97	178.8 ±5.6	-0.99 ± 0.02	...	37.6e-6 ± 0.7e-6	8-1000	10210
091208410	1.063	15	144.2 ±15	-1.48 ± 0.05	...	5.8e-6 ± 0.2e-6	8-1000	(10263) 10266
091221870	...	32	207 ±20	-0.69 ± 0.07	-2.3 ± 0.25	1.38e-5 ± 0.05e-5	8-1000	10293
100111176	...	12	...	-1.66 ± 0.05	...	1.5e-6 ± 0.1e-6	8-1000	10319
100117879	...	0.4	287 ±60	-0.14 ± 0.3	...	4.1e-7 ± 0.5e-7	8-1000	10345
100122616	...	6.6	45.6 ±1.5	-0.98 ± 0.05	-2.31± 0.03	1.0e-5 ± 1.0e-7	8-1000	10355
100130729	...	106	100.5 ±4.77	-0.97 ± 0.06	...	8.21e-6 ± 0.3e-6	8-1000	10372
100130777	...	90	208 ±17.1	-1.22 ± 0.04	...	1.342e-5 ± 0.047e-5	8-1000	10373
100131730	...	6.2	132.10 ±6.28	-0.63 ± 0.05	-2.21± 0.05	7.723e-6 ± 0.13e-6	8-1000	10358
100205490	...	13.6	124.2 ±14	-0.47 ± 0.2	...	1.41e-6 ± 0.082e-6	8-1000	10397
100206563	...	0.13	439 ±66	-0.09 ± 0.16	-2.35± 0.32	9.3e-7 ± 0.4e-7	8-1000	10381
100212588	...	2.3	159.3 ±45.1	-1.15 ± 0.2	...	3.81e-7 ± 0.06e-7	8-1000	10406
100218194	...	30.8	131.6 ±26	-0.14 ± 0.35	-2 ± 0.22	2.58e-6 ± 0.21e-6	8-1000	10431
100223110	...	0.206	1143 ±109	-0.31 ± 0.08	...	1.42e-6 ± 0.04e-6	8-1000	10448
100224112	...	77	181.4 ±27	-1.36 ± 0.07	...	1.08e-5 ± 0.05e-5	8-1000	10457
100225115	...	13	428 ±110	-0.72 ± 0.13	-2.15± 0.5	7.6e-6 ± 0.3e-6	8-1000	10449
100322045	...	37	309 ±16	-0.88 ± 0.02	-2.15± 0.05	6.13e-5 ± 0.04e-5	10-1000	10539
100325275	...	8.3	159.3 ±12	-0.45 ± 0.12	...	1.99e-6 ± 0.04e-6	8-1000	10546

Notes. * References in brackets are for the redshift. (a) Greiner J., Clemens C., Kruhler T. et al. 2009, A&A, 498, 89; (b) R. Salvaterra et al., 2009, Nature, 461, 1258.